Deutsche Forschungsgemeinschaft
Priority Programme 1962

Monotone Multilevel for FOSLS Linear Elastic Contact

Gabriele Rovi, Bernhard Kober, Gerhard Starke, Rolf Krause

SPP 1962 | Non-smooth and Complementarity-based Distributed Parameter Systems: Simulation and Hierarchical Optimization

Preprint Number SPP1962-105

received on February 25, 2019

Edited by
SPP1962 at Weierstrass Institute for Applied Analysis and Stochastics (WIAS)
Leibniz Institute in the Forschungsverbund Berlin e.V.
Mohrenstraße 39, 10117 Berlin, Germany
E-Mail: spp1962@wias-berlin.de

World Wide Web: http://spp1962.wias-berlin.de/

Monotone multilevel for FOSLS linear elastic contact

Gabriele Rovi*[1], Bernhard Kober†[2], Gerhard Starke‡[2], and Rolf Krause§[1]

[1]Institute of Computational Science, Università della Svizzera italiana, Via Giuseppe Buffi 13, 6900, Lugano, Switzerland
[2]Fakultät für Mathematik, Universität Duisburg-Essen, Thea-Leymann-Straße 9, 45127 Essen, Germany

February 19, 2019

Abstract

The first order system least-squares for linear ealstic contact problems is examined. The complementarity term is added to the functional, while the local inequality constraints are inserted in the definition of the convex set. A mixed formulation for both displacement and stress, subject to the contact conditions, is consequently obtained. This holds for both compressible and incompressible materials. The problem is then discretized by continuous piecewise linear functions for the displacement and by the lowest order Raviart-Thomas for the stress. As a solver, a multilevel method is exploited and in particular, due to the local constraints, a monotone multilevel method. A linear convergence rate in the limit case is finally shown in numerical experiments.

1 Introduction

The least-squares system of first order equations (FOSLS) for linear elasticity has been developed in [12], by introducing a functional which is the sum of the squared L^2 norms of the residuals of the equilibrium and constitutive equations ([1], [10]). In this way, displacement $\mathbf{u} \in H^1(\Omega)$ and stress $\boldsymbol{\sigma} \in H(\mathrm{div}, \Omega)$ are considered as independent, giving rise to a mixed weak form. With respect to the standard primal displacement formulation, several are the advantages of this approach. First, the stress can be directly accessed, which can make the treatment of the elasto-plasticity (see [27]) and friction cases easier. Second, the Lamé

*rovig@usi.ch
†bernhard.kober@uni-due.de
‡gerhard.starke@uni-due.de
§rolf.krause@usi.ch

parameters are not restricted to a limited range of values: indeed, incompressible solids can be treated with no additional effort. Third, the least-squares functional is a reliable and efficient a posteriori error estimator. All these properties suggested the generalization of [12] to contact, as shown in [23] for the Signorini's problem. The respective discretization is carried out by conforming finite element spaces: continuouse piecewise linear functions for the displacement and Raviart-Thomas elements of the lowest order for the stress.
Different tecniques for solving the constrained optimisation problem, which describes the Signorini problem in the displacement formulation, have been proposed. A typical one is the projected Gauß-Seidel, whose behaviour unfortunately deteriorates by increasing the size of the problem. Therefore multilevel approaches are preferred. Here we want to extend to the least-squares setting the monotone multilevel exposed in [21], [22], [24], while for the other methods we refer the reader to the citations therein (for example [8], [15], [25]). Peculiarly, the monotone multilevel aims to compute the solution of the discrete problem by adding to the current iterate fine and coarse corrections that actually minimize the energy functional. Effectively the framework of the least-squares linear elasticity for contact problem perfectly adapts to this case. Investigating this strategy is actually the main goal of the present paper. Nevertheless the primal and the dual variables belong to different spaces, i.e $\mathbf{u} \in H^1(\Omega)$ and $\boldsymbol{\sigma} \in H(\mathrm{div}, \Omega)$. And since $H^1 \subset H(\mathrm{div}, \Omega)$, schemes applied to the primal case cannot be transferred straightforwardly to the mixed one.
The most important difference between $H(\mathrm{div}, \Omega)$ and $H^1(\Omega)$ consists in the kernels of the divergence, which contains all divergence-free functions, and of the gradient, which consists only of constants. Between the two, the kernel of the gradient operator is smaller and its elements can be well represented on coarse meshes. On the other hand, the kernel of the divergence is very large and its functions can have large gradients, so that their representation on coarse meshes can be very poor. In order to circumvent this drawback, some variants of multilevel methods for $H(\mathrm{div}, \Omega)$ have been studied, at least for the linear case. A general overview can be found in [28]. In [16] a geometric multigrid has been proposed. Then in [17] and [19] a more general framework for dealing algebraic and geometric multigrid has been developed. All these approaches are based on the Helmoltz decomposition, which is a tool used not only in theory but also in the implementation. In particular, the different components in the Helmoltz decomposition can be expressed as functions of certain potentials, which are tackled separately. To this aim, various projections into the potential spaces are needed. However in this paper we take advantage of the work proposed in [2], [3], [4]. In this way, no potential space has to be considered, although a proper patch smoother is required. Moreover this smoother can be extended to the least-squares formulation as proposed in [26]. In this way, we tackle all together not only the different components of the Helmoltz decomposition for the stress, but also the displacement. The price to pay is the solution of local problems which can be larger with respect to the standard ones.
So far, to the authors' knowledge, only multilevel methods for linear FOSLS problems have been discussed. Nevertheless the Signorini's problem is non-linear. Of course by exploiting the active set method, for each arising linear problem, a linear multilevel method could be

used. However in this way the non-linearities would not appear into the multilevel cycles, but only in the external active set. The main advantage of a monotone multilevel method is that it is able to deal with constraints inside the multilevel cycle itself. In the primal case, it has been shown in [20] that, when the number of iterations $k \to \infty$, all the active degrees of freedom are detected, the inequality constraints become equalities and the overall problem is reduced to a linear one. In such a situation, a linear convergence rate can be shown. Altough this formula is independent of the meshwidth, it depends on the number of levels J of the multilevel method. Some years later (see [5], [6], [7]) the same kind of behaviour has been prooved for all the iterations, and not only in the limit case.
In this paper the primal case is generalized to the FOSLS for contact problems and some numerical experiments will be carried out to show that the linear rate is meaningful also in this situation. The article is organized in the following way. In the second section, we introduce the problem. In the third one, existence and uniqueness of the solution are shown. In the fourth section a monotone multilevel strategy is proposed, while in the fifth one some non-linear projection operators for the constraints are introduced. In the sixth section, proper truncated multilevel basis are discussed. Finally in the last section some numerical experiments are presented.

2 Definition of the problem

In this section the strong formulations of linear elasticity and linear elastic contact for dimension $d = 2, 3$ are introduced . Different weak formulations are discussed, with their advantages and disadvantages. The main focus of this paper regards the FOSLS formulation for contact. Therefore the LS functional for linear elasticity and the augmented variant for contact problems are defined.
Let a body be reprented by Ω, an open, bounded, connected subset of $\mathbb{R}^d$, where $d = 2, 3$ is the dimension of the problem. The boundary $\partial\Omega$, Lipschitz and continuous, is the union of two open disjoint subsets $\partial\Omega = \Gamma_D \cup \Gamma_N$, with $\Gamma_D \neq \emptyset$ and $\Gamma_D \cap \Gamma_N = \emptyset$. Then let $\mathbf{f} = (f_1, ..., f_d)^T$ be the body force, $\mathbf{u} = (u_1, ..., u_d)^T$ the displacement field, $\boldsymbol{\sigma} = (\sigma_{ij})_{d\times d}$ the stress tensor. By bold symbols we denote vectors or tensors. We use bold letters for
The *strong formulation of linear elasticity* is the following: *find* $\boldsymbol{u}$, $\boldsymbol{\sigma}$ *such that*:

$$\begin{cases} \mathrm{div}\boldsymbol{\sigma} + \mathbf{f} = 0 & \Omega \quad \text{momentum balance equation} \\ \boldsymbol{\mathcal{A}}\boldsymbol{\sigma} - \boldsymbol{\varepsilon}(\mathbf{u}) = 0 & \Omega \quad \text{constitutive law} \\ \mathbf{u} = \mathbf{u}^D & \Gamma_D \quad \text{Dirichlet BC} \\ \boldsymbol{\sigma}\mathbf{n} = \mathbf{t}^N & \Gamma_N \quad \text{Neumann BC} \end{cases}$$

where the linearized strain tensor $\boldsymbol{\varepsilon}(\mathbf{u}) = \mathrm{sym}(\nabla\mathbf{u})$ is the symmetric part of the displacement gradient, $\boldsymbol{\mathcal{A}} = \dfrac{1}{2\mu}\left(\boldsymbol{\sigma} - \dfrac{\lambda}{d\lambda + 2\mu}\mathrm{tr}\boldsymbol{\sigma}\mathbf{I}\right)$ is the compliance tensor with tr, d, λ and μ denoting respectively the trace operator, the dimension of the problem and the Lamé

parameters.
Now let Γ_C be the contact boundary such that $\partial\Omega = \Gamma_C \cup \Gamma_D \cup \Gamma_N$, $\Gamma_i \cap \Gamma_j = \emptyset$ for $i, j = D, N, C, i \neq j$, and $\Gamma_D \neq \emptyset$. Then, by adding the following constraints:

$$\begin{cases} \mathbf{u} \cdot \mathbf{n}_o - g \leq 0 & \Gamma_C \quad \text{impenetrability} \\ (\boldsymbol{\sigma}\mathbf{n}) \cdot \mathbf{n}_o \leq 0 & \Gamma_C \quad \text{direction of the surface pressure} \\ (\mathbf{u} \cdot \mathbf{n}_o - g)\,((\boldsymbol{\sigma}\mathbf{n}) \cdot \mathbf{n}_o) = 0 & \Gamma_C \quad \text{complementarity condition} \\ (\boldsymbol{\sigma}\mathbf{n}) \cdot \mathbf{t}_o = 0 & \Gamma_C \quad \text{frictionless condition} \end{cases}$$

the strong formulation of contact for linear elasticity is finally obtained. Here $\mathbf{n}$ represents the outward normal of the body, while $\mathbf{n}_o$ and $\mathbf{t}_o$ respectively represent the normal and the tangent vectors of the obstacle. The gap function g is instead the distance in the normal direction between the obstacle and the body. Here the first condition means that no penetration can occur between the body and the obstacle. The second condition implies that, whenever contact forces arise, they have to be of compression and no adhesion is permitted. The third condition is a classic complementarity condition of the first two. The last one states that only normal stresses can arise. Finally, by confusing the normal and the tangent vectors of the obstacle with the ones of the body, i.e. $\mathbf{n} \approx \mathbf{n}_o$ and $\mathbf{t} \approx \mathbf{t}_o$, the linearized contact formulation for linear elasticity is recovered (see [18]).
In general, from the strong formulation of the contact linear elasticity, different variants of weak forms can be derived. In the following, a list of motivations that retraces the one in [12] is presented. By substituing the constitutive equation ($\boldsymbol{\sigma} = \mathcal{C}\boldsymbol{\varepsilon}(\mathbf{u})$, with $\mathcal{C} = \boldsymbol{\mathcal{A}}^{-1}$ the elasticity tensor) into the momentum balance one, the displacement formulation is consequently obtained. The displacement $\mathbf{u}$, belonging to $H^1(\Omega)$, is the only unknown and the stress $\boldsymbol{\sigma}$, belonging only to $L^2(\Omega)$, is derived *a posteriori* and cannot be carefully approximated. Furthermore locking phenomena can arise for incompressible or nearly incompressible solids ($\lambda \gg 1$ or $\lambda \to \infty$).
To achieve a better approximation of the stress, the mixed formulation by Hellinger-Reissner can be used ([11]). Given the energy-functional $\mathcal{J}(\mathbf{u}, \boldsymbol{\sigma}) = \frac{1}{2}(\boldsymbol{\mathcal{A}}\boldsymbol{\sigma}, \boldsymbol{\sigma})_{L^2(\Omega)} + (\nabla \cdot \boldsymbol{\sigma} + \mathbf{f}, \mathbf{u})_{L^2(\Omega)}$, both displacement and stress $(\mathbf{u}, \boldsymbol{\sigma})$ are unknowns of the problem, respectively belonging to $L^2(\Omega)^d \times H_{\mathrm{div},S}(\Omega)^d$, where $H_{\mathrm{div},S}(\Omega)^d$ is the space of symmetric tensors in $H_{\mathrm{div}}(\Omega)$. In this case, in order to satisfy the inf-sup condition in the discrete setting, a stable combination of finite element spaces is needed. Although such spaces have been built ([12]), the number of degrees of freedom they require is very large. Furthermore the corresponding linear system is a saddle point problem, that in general is difficult to solve.
The approach that is here presented is based on the LS principle ([9], [10], [29]). The main idea behind it is to build a fictitious functional as the weighted sum of the squared L^2-norms of the residual equations. Unlike the previous cases, now it is required more regularity on both variables: $\mathbf{u} \in H^1(\Omega)$, $\boldsymbol{\sigma} \in H(\mathrm{div}, \Omega)$. With respect to the Hellinger-Reissner formulation, the symmetry of the stress tensor is not demanded. Indeed, as it is shown in [12], $\left\|\boldsymbol{\sigma} - \boldsymbol{\sigma}^T\right\|_{L^2(\Omega)} \leq C \left\|\boldsymbol{\mathcal{A}}\boldsymbol{\sigma} - \boldsymbol{\varepsilon}(\mathbf{u})\right\|_{L^2(\Omega)}$. Thus, by reducing the residual of the constitutive law, the asymmetry is reduced as well. Principally, spaces that would be useful for the

analysis are the following:

$$H^1_D(\Omega) = \left\{ \mathbf{v} \in \left[H^1(\Omega)\right]^d, \quad \mathbf{v}|_{\Gamma_D} = \mathbf{u}^D \text{ on } \Gamma_D \right\} \qquad H^1_{D,0}(\Omega) = \left\{ \mathbf{v} \in \left[H^1(\Omega)\right]^d, \quad \mathbf{v}|_{\Gamma_D} = \mathbf{0} \text{ on } \Gamma_D \right\}$$

$$H_N(\mathrm{div}, \Omega) = \left\{ \boldsymbol{\tau} \in [H(, \mathrm{div}, \Omega)]^d, \quad \boldsymbol{\tau}\mathbf{n}|_{\Gamma_N} = \mathbf{t}^N \text{ on } \Gamma_N \right\} \quad H_{N,0}(\mathrm{div}, \Omega) = \left\{ \boldsymbol{\tau} \in [H(, \mathrm{div}, \Omega)]^d, \quad \boldsymbol{\tau}\mathbf{n}|_{\Gamma_N} = \mathbf{0} \text{ on } \Gamma_N \right\}$$

Then, relying on the formulation given in [23], we define the linear elasticity LS functional $\mathcal{F}$ and the corresponding augmented LS functional $\mathcal{J}$ for contact:

$$\mathcal{F}(\mathbf{u}, \boldsymbol{\sigma}; \mathbf{f}) = C_{\text{eq}} \left\| \mathrm{div}\boldsymbol{\sigma} + \mathbf{f} \right\|^2_{L^2(\Omega)^d} + C_{\text{const}} \left\| \boldsymbol{\mathcal{A}}\boldsymbol{\sigma} - \boldsymbol{\varepsilon}(\mathbf{u}) \right\|^2_{L^2(\Omega)^d} \tag{1}$$

$$\mathcal{J}(\mathbf{u}, \boldsymbol{\sigma}; \mathbf{f}, g) = \mathcal{F}(\mathbf{u}, \boldsymbol{\sigma}; \mathbf{f}) + C_{\text{compl}} \langle \mathbf{u} \cdot \mathbf{n} - g, (\boldsymbol{\sigma}\mathbf{n}) \cdot \mathbf{n} \rangle_{\Gamma_C} \tag{2}$$

So that the problem can be formulated in this way: find $(\mathbf{u}, \boldsymbol{\sigma})$ such that

$$\begin{aligned} (\mathbf{u}, \boldsymbol{\sigma}) &= \underset{(\mathbf{u},\boldsymbol{\sigma}) \in K}{\arg\min}\, \mathcal{J}(\mathbf{u}, \boldsymbol{\sigma}; \mathbf{f}, g) \\ K &= \left\{ (\mathbf{u}, \boldsymbol{\sigma}) \in H^1_D(\Omega) \times H_N(\mathrm{div}, \Omega) : \quad \mathbf{u} \cdot \mathbf{n} - g \leq 0, \ (\boldsymbol{\sigma}\mathbf{n}) \cdot \mathbf{n} \leq 0, \ (\boldsymbol{\sigma}\mathbf{n}) \cdot \mathbf{t} = \mathbf{0} \text{ on } \Gamma_C \right\} \end{aligned} \tag{3}$$

The complementarity condition on Γ_C is a non-linear term. Defining the convex set K by adding also this requirement would be cumbersome, at least from a computational perspective. On the other hand, augmenting the functional with this term seems a more natural choice. Of course in the discrete setting, due to the fact that we do not enforce it strongly and we just add it as a penalty addendum, the complementarity condition will be not fulfilled exactly and so will be only approximated.
The augmented functional $\mathcal{J}(\mathbf{u}, \boldsymbol{\sigma}; \mathbf{f}, g)$ is Gateaux-differentiable and strongly convex, as we will show. Therefore the problem (3) can be reformulated in the following way: find $(\mathbf{u}, \boldsymbol{\sigma}) \in K$ such that $\forall (\mathbf{v}, \boldsymbol{\tau}) \in K$:

$$\begin{cases} \left\langle \dfrac{\partial \mathcal{J}(\mathbf{u}, \boldsymbol{\sigma}; \mathbf{f}, g)}{\partial \mathbf{u}}, \mathbf{v} - \mathbf{u} \right\rangle = -2 \left(\boldsymbol{\sigma} - \boldsymbol{\varepsilon}(\mathbf{u}), \boldsymbol{\varepsilon}(\mathbf{v} - \mathbf{u}) \right) + \langle \mathbf{n} \cdot (\boldsymbol{\sigma}\mathbf{n}), \mathbf{n} \cdot (\mathbf{v} - \mathbf{u}) \rangle_{\Gamma_C} \geq 0 \\ \left\langle \dfrac{\partial \mathcal{J}(\mathbf{u}, \boldsymbol{\sigma}; \mathbf{f}, g)}{\partial \boldsymbol{\sigma}}, \boldsymbol{\tau} - \boldsymbol{\sigma} \right\rangle = 2 \left(\mathrm{div}\, \boldsymbol{\sigma} + \mathbf{f}, \mathrm{div}(\boldsymbol{\tau} - \boldsymbol{\sigma}) \right) + 2 \left(\boldsymbol{\sigma} - \boldsymbol{\varepsilon}(\mathbf{u}), \boldsymbol{\tau} - \boldsymbol{\sigma} \right) + \langle \mathbf{n} \cdot \mathbf{u} - g, \mathbf{n} \cdot (\boldsymbol{\tau} - \boldsymbol{\sigma})\, \mathbf{n} \rangle_{\Gamma_C} \geq 0 \end{cases} \tag{4}$$

Here and in the following, whenever the dot product or the norm is not explicitly defined, it is assumed to be L^2 on the domain Ω, i.e $(\cdot, \cdot) = (\cdot, \cdot)_{L^2(\Omega)}$ and $\|\cdot\| = \|\cdot\|_{L^2(\Omega)}$.

3 Existence and uniqueness of the solution

Standard FOSLS functionals are simply positive definite quadratic forms. Thus they are also strongly convex and differentiable, so that the existence and uniqueness of the minimizer immediately follows. In (2) the inconvenience is represented by the complementarity

term, which is not convex in general. Therefore it is not clear whether the whole functional is still convex or not and if such convexity can depend on the weights in front of each term. Actually, by showing some intermediate results, we can prove the strong convexity of the functional for non homogeneous boundary conditions, which together with the continuity of the functional implies the existence and uniqueness of the solution $(\mathbf{u}, \boldsymbol{\sigma})$. From the proof we can see that the choice of the constants C_{const}, C_{eq}, C_{compl} plays an important role.
Let us define the following squared norm $M(\mathbf{s}, \mathbf{w}) : H^1_D(\Omega) \times H_N(\text{div}, \Omega) \to \mathbb{R}$ by:

$$M(\mathbf{s}, \mathbf{w}) = \|\boldsymbol{\varepsilon}(\mathbf{w})\|^2_{L^2} + \|\mathbf{s}\|^2_{H_{\text{div}}} = \|\boldsymbol{\varepsilon}(\mathbf{w})\|^2_{L^2} + \|\mathbf{s}\|^2_{L^2} + \|\text{div}\, \mathbf{s}\|^2_{L^2}$$

Then we can prove:

Lemma 3.1. *Given $\boldsymbol{u}, \boldsymbol{v} \in H^1_D(\Omega)$ and $\boldsymbol{\sigma}, \boldsymbol{\tau} \in H_N(\text{div}, \Omega)$, let $\boldsymbol{w} = \boldsymbol{u} - \boldsymbol{v}$ and $\boldsymbol{s} = \boldsymbol{\sigma} - \boldsymbol{\tau}$. Then there exist two positive constants, $C_1 > 0$ and $C_2 > 0$, such that:*

$$M(\boldsymbol{s}, \boldsymbol{w})C_1 \leq \mathcal{J}(\boldsymbol{w}, \boldsymbol{s}; 0, 0) \leq C_2 M(\boldsymbol{s}, \boldsymbol{w}). \tag{5}$$

Proof. The proof is similar to the Theorem 3.1 in [12]. The upper bound can be easily shown by using $\|\boldsymbol{\mathcal{A}}\boldsymbol{\tau}\| \leq \dfrac{1}{2\mu}\|\boldsymbol{\tau}\|$, the triangle, Young and trace inequalities.
In order to prove the lower estimate, it is sufficient to bound all the terms in M with the functional. Knowing that $\|\boldsymbol{\mathcal{A}}\boldsymbol{\tau}\| \leq \dfrac{1}{2\mu}\|\boldsymbol{\tau}\|$ and $(\boldsymbol{\mathcal{A}}\mathbf{s}, \mathbf{s}) \geq \dfrac{1}{2\mu}\|\mathbf{s}\|^2$, we get:

$$\begin{aligned}
\|\mathbf{s}\|^2 + \|\text{div}\, \mathbf{s}\|^2 + \|\boldsymbol{\varepsilon}(\mathbf{w})\|^2 \leq & \|\mathbf{s}\|^2 + \|\text{div}\, \mathbf{s}\|^2 + 2\|\boldsymbol{\varepsilon}(\mathbf{w}) - \boldsymbol{\mathcal{A}}\mathbf{s}\|^2 + 2\|\boldsymbol{\mathcal{A}}\mathbf{s}\|^2 && (6)\\
\leq & \left(\frac{2\mu^2 + 1}{2\mu^2}\right)\|\mathbf{s}\|^2 + \|\text{div}\, \mathbf{s}\|^2 + 2\|\boldsymbol{\varepsilon}(\mathbf{w}) - \boldsymbol{\mathcal{A}}\mathbf{s}\|^2 && (7)\\
\leq & \left(\frac{2\mu^2 + 1}{\mu}\right)(\boldsymbol{\mathcal{A}}\mathbf{s}, \mathbf{s}) + \|\text{div}\, \mathbf{s}\|^2 + 2\|\boldsymbol{\varepsilon}(\mathbf{w}) - \boldsymbol{\mathcal{A}}\mathbf{s}\|^2 && (8)
\end{aligned}$$

Thus it is now sufficient to bound $\dfrac{2\mu^2 + 1}{2\mu^2}(\boldsymbol{\mathcal{A}}\mathbf{s}, \mathbf{s})$. By exploiting the Green's formula, $\left\|\mathbf{s} - \mathbf{s}^T\right\| \leq 4\mu\|\boldsymbol{\mathcal{A}}\mathbf{s} - \boldsymbol{\varepsilon}(\mathbf{w})\|$ and Poincaré's and Korn's inequalities, respectively with con-

stants C_p and K, we get:

$$
\begin{aligned}
(\boldsymbol{\mathcal{A}}\mathbf{s},\mathbf{s}) &= (\boldsymbol{\mathcal{A}}\mathbf{s}-\boldsymbol{\varepsilon}(\mathbf{w}),\mathbf{s})+(\boldsymbol{\varepsilon}(\mathbf{w}),\mathbf{s}) = (\boldsymbol{\mathcal{A}}\mathbf{s}-\boldsymbol{\varepsilon}(\mathbf{w}),\mathbf{s})+(\mathbf{s}-\frac{1}{2}\left(\mathbf{s}-\mathbf{s}^T\right),\nabla\mathbf{w}) \\
&= (\boldsymbol{\mathcal{A}}\mathbf{s}-\boldsymbol{\varepsilon}(\mathbf{w}),\mathbf{s})-(\mathrm{div}\mathbf{s},\mathbf{w})-\frac{1}{2}\left(\mathbf{s}-\mathbf{s}^T,\nabla\mathbf{w}\right)+\int_{\partial\Omega}\mathbf{s}\mathbf{n}\cdot\mathbf{w} \\
&\leq \|\boldsymbol{\mathcal{A}}\mathbf{s}-\boldsymbol{\varepsilon}(\mathbf{w})\|\|\mathbf{s}\|+\|\mathrm{div}\mathbf{s}\|\|\mathbf{w}\|+\frac{1}{2}\left\|\mathbf{s}-\mathbf{s}^T\right\|\|\nabla\mathbf{w}\|+\int_{\partial\Omega}\mathbf{s}\mathbf{n}\cdot\mathbf{w} \\
&\leq \|\boldsymbol{\mathcal{A}}\mathbf{s}-\boldsymbol{\varepsilon}(\mathbf{w})\|\|\mathbf{s}\|+\max\{1,C_p\}\|\mathbf{w}\|\left(\|\mathrm{div}\mathbf{s}\|+\frac{1}{2}\left\|\mathbf{s}-\mathbf{s}^T\right\|\right)+\int_{\partial\Omega}\mathbf{s}\mathbf{n}\cdot\mathbf{w} \\
&\leq \|\boldsymbol{\mathcal{A}}\mathbf{s}-\boldsymbol{\varepsilon}(\mathbf{w})\|\|\mathbf{s}\|+\max\{1,C_p\}K\|\boldsymbol{\varepsilon}(\mathbf{w})\|\left(\|\mathrm{div}\mathbf{s}\|+2\mu\|\boldsymbol{\mathcal{A}}\mathbf{s}-\boldsymbol{\varepsilon}(\mathbf{w})\|\right)+\int_{\partial\Omega}\mathbf{s}\mathbf{n}\cdot\mathbf{w} \\
&\leq \|\boldsymbol{\mathcal{A}}\mathbf{s}-\boldsymbol{\varepsilon}(\mathbf{w})\|\|\mathbf{s}\|+\tilde{K}\|\boldsymbol{\varepsilon}(\mathbf{w})\|\mathrm{div}\mathbf{s}\|+2\mu\tilde{K}\|\boldsymbol{\varepsilon}(\mathbf{w})\|\|\boldsymbol{\mathcal{A}}\mathbf{s}-\boldsymbol{\varepsilon}(\mathbf{w})\|+\int_{\partial\Omega}\mathbf{s}\mathbf{n}\cdot\mathbf{w}
\end{aligned}
$$

Where we have defined $\tilde{K}=\max\{1,C_p\}K$. Applying Young's inequalities three times, with parameters $\alpha,\ \beta,\ \gamma>0$, we obtain:

$$
\begin{aligned}
(\boldsymbol{\mathcal{A}}\mathbf{s},\mathbf{s}) \leq & \frac{1}{4\alpha}\|\boldsymbol{\mathcal{A}}\mathbf{s}-\boldsymbol{\varepsilon}(\mathbf{w})\|^2+\alpha\|\mathbf{s}\|^2+\tilde{K}\beta\|\boldsymbol{\varepsilon}(\mathbf{w})\|^2+\frac{\tilde{K}}{4\beta}\|\mathrm{div}\mathbf{s}\|^2+... \\
& 2\mu\tilde{K}\gamma\|\boldsymbol{\varepsilon}(\mathbf{w})\|^2+\frac{\mu\tilde{K}}{2\gamma}\|\boldsymbol{\mathcal{A}}\mathbf{s}-\boldsymbol{\varepsilon}(\mathbf{w})\|^2+\int_{\partial\Omega}\mathbf{s}\mathbf{n}\cdot\mathbf{w} \\
= & \left(\frac{1}{4\alpha}+\frac{\mu\tilde{K}}{2\gamma}\right)\|\boldsymbol{\mathcal{A}}\mathbf{s}-\boldsymbol{\varepsilon}(\mathbf{w})\|^2+\left(\tilde{K}\beta+2\mu\tilde{K}\gamma\right)\|\boldsymbol{\varepsilon}(\mathbf{w})\|^2+... \\
& +\alpha\|\mathbf{s}\|^2+\frac{\tilde{K}}{4\beta}\|\mathrm{div}\mathbf{s}\|^2+\int_{\partial\Omega}\mathbf{s}\mathbf{n}\cdot\mathbf{w}.
\end{aligned}
$$

Thus we reuse the same argument of (6) and collect the common terms:

$$
\begin{aligned}
(\boldsymbol{\mathcal{A}}\mathbf{s},\mathbf{s}) \leq & \left(\frac{1}{4\alpha}+\frac{\mu\tilde{K}}{2\gamma}\right)\|\boldsymbol{\mathcal{A}}\mathbf{s}-\boldsymbol{\varepsilon}(\mathbf{w})\|^2+\left(\tilde{K}\beta+2\mu\tilde{K}\gamma\right)\left(2\|\boldsymbol{\mathcal{A}}\mathbf{s}-\boldsymbol{\varepsilon}(\mathbf{w})\|^2+2\|\boldsymbol{\mathcal{A}}\mathbf{s}\|^2\right)+... \\
& +\alpha\|\mathbf{s}\|^2+\frac{\tilde{K}}{4\beta}\|\mathrm{div}\mathbf{s}\|^2+\int_{\partial\Omega}\mathbf{s}\mathbf{n}\cdot\mathbf{w} \\
= & \left(\frac{1}{4\alpha}+\frac{\mu\tilde{K}}{2\gamma}+2\tilde{K}\beta+4\mu\tilde{K}\gamma\right)\|\boldsymbol{\mathcal{A}}\mathbf{s}-\boldsymbol{\varepsilon}(\mathbf{w})\|^2+\left(2\tilde{K}\beta+4\mu\tilde{K}\gamma\right)\|\boldsymbol{\mathcal{A}}\mathbf{s}\|^2+... \\
& +\alpha\|\mathbf{s}\|^2+\frac{\tilde{K}}{4\beta}\|\mathrm{div}\mathbf{s}\|^2+\int_{\partial\Omega}\mathbf{s}\mathbf{n}\cdot\mathbf{w}.
\end{aligned}
$$

Finally by exploiting $\|\boldsymbol{\mathcal{A}}\mathbf{s}\|^2 \leq \frac{1}{4\mu^2}\|\mathbf{s}\|^2 \leq \frac{1}{2\mu}(\boldsymbol{\mathcal{A}}\mathbf{s},\mathbf{s})$, we get:

$$
\begin{aligned}
(\boldsymbol{\mathcal{A}}\mathbf{s},\mathbf{s}) &\leq \left(\frac{1}{4\alpha}+\frac{\mu\tilde{K}}{2\gamma}+2\tilde{K}\beta+4\mu\tilde{K}\gamma\right)\|\boldsymbol{\mathcal{A}}\mathbf{s}-\boldsymbol{\varepsilon}(\mathbf{w})\|^2+\left(2\tilde{K}\beta+4\mu\tilde{K}\gamma\right)\frac{1}{2\mu}(\boldsymbol{\mathcal{A}}\mathbf{s},\mathbf{s})+\ldots\\
&\quad+2\mu\alpha(\boldsymbol{\mathcal{A}}\mathbf{s},\mathbf{s})+\frac{\tilde{K}}{4\beta}\|\mathrm{div}\mathbf{s}\|^2+\int_{\partial\Omega}\mathbf{s}\mathbf{n}\cdot\mathbf{w}\\
&=\left(\frac{1}{4\alpha}+\frac{\mu\tilde{K}}{2\gamma}+2\tilde{K}\beta+4\mu\tilde{K}\gamma\right)\|\boldsymbol{\mathcal{A}}\mathbf{s}-\boldsymbol{\varepsilon}(\mathbf{w})\|^2+\left[\left(2\tilde{K}\beta+4\mu\tilde{K}\gamma\right)\frac{1}{2\mu}+2\mu\alpha\right](\boldsymbol{\mathcal{A}}\mathbf{s},\mathbf{s})+\ldots\\
&\quad+\frac{\tilde{K}}{4\beta}\|\mathrm{div}\mathbf{s}\|^2+\int_{\partial\Omega}\mathbf{s}\mathbf{n}\cdot\mathbf{w}.
\end{aligned}
$$

Now by letting $\alpha=\frac{1}{8\mu}$, $\beta=\frac{\mu}{8\tilde{K}}$, $\gamma=\frac{1}{16\tilde{K}}$, it follows that:

$$
\begin{aligned}
\left[\left(2\tilde{K}\beta+4\mu\tilde{K}\gamma\right)\frac{1}{2\mu}+2\mu\alpha\right]&=\frac{1}{2}\\
\left(\frac{1}{4\alpha}+\frac{\mu\tilde{K}}{2\gamma}+2\tilde{K}\beta+4\mu\tilde{K}\gamma\right)&=\frac{5}{2}\mu+8\mu\tilde{K}^2.
\end{aligned}
$$

Therefore by enforcing the boundary conditions $\mathbf{w}|_{\Gamma_D}=\mathbf{0}$, $\mathbf{sn}|_{\Gamma_N}=\mathbf{0}$, $(\mathbf{sn})\cdot\mathbf{t}|_{\Gamma_C}=0$, we get:

$$
(\boldsymbol{\mathcal{A}}\mathbf{s},\mathbf{s})\leq\left(5\mu+16\mu\tilde{K}^2\right)\|\boldsymbol{\mathcal{A}}\mathbf{s}-\boldsymbol{\varepsilon}(\mathbf{w})\|^2+\frac{4\tilde{K}^2}{\mu}\|\mathrm{div}\mathbf{s}\|^2+2\langle\mathbf{sn}\cdot\mathbf{n},\mathbf{w}\cdot\mathbf{n}\rangle_{\Gamma_C}. \tag{9}
$$

Combining (8) and (9):

$$
\begin{aligned}
\|\mathbf{s}\|^2+\|\mathrm{div}\,\mathbf{s}\|^2+\|\boldsymbol{\varepsilon}(\mathbf{w})\|^2 &\leq \left(\frac{2\mu^2+1}{\mu}\right)(\boldsymbol{\mathcal{A}}\mathbf{s},\mathbf{s})+\|\mathrm{div}\,\mathbf{s}\|_{L^2}^2+2\|\boldsymbol{\varepsilon}(\mathbf{w})-\boldsymbol{\mathcal{A}}\mathbf{s}\|^2\\
&\leq\left(1+\left(\frac{2\mu^2+1}{\mu}\right)\frac{4\tilde{K}^2}{\mu}\right)\|\mathrm{div}\,\mathbf{s}\|^2+\ldots\\
&\quad\left(2+\left(\frac{2\mu^2+1}{\mu}\right)\left(5\mu+16\mu\tilde{K}^2\right)\right)\|\boldsymbol{\varepsilon}(\mathbf{w})-\boldsymbol{\mathcal{A}}\mathbf{s}\|^2+\ldots\\
&\quad 2\left(\frac{2\mu^2+1}{\mu}\right)\langle\mathbf{sn}\cdot\mathbf{n},\mathbf{w}\cdot\mathbf{n}\rangle_{\Gamma_C}
\end{aligned}
$$

Therefore the inequality from below is fulfilled with constants:

$$
\begin{aligned}
C_1 &= \frac{1}{2\left(\frac{2\mu^2+1}{\mu}\right)} & C_{\text{compl}} &= 1 \\
C_{\text{eq}} &\geq \frac{\left(1+\left(\frac{2\mu^2+1}{\mu}\right)\frac{4\tilde{K}^2}{\mu}\right)}{2\left(\frac{2\mu^2+1}{\mu}\right)} & C_{\text{const}} &\geq \frac{\left(2+\left(\frac{2\mu^2+1}{\mu}\right)\left(5\mu+16\mu\tilde{K}^2\right)\right)}{2\left(\frac{2\mu^2+1}{\mu}\right)}
\end{aligned}
\tag{10}
$$

Remark:
In contrast to the proof of Theorem 3.1 in [12], we define the functional $\mathcal{J}$ only with the L^2 norms of the residuals, not considering the case of the H^{-1} norm. ■

Lemma 3.2. *For constants satisfying (10), the augmented LS functional is strongly convex.*

Proof. The functional $\mathcal{F}(\mathbf{u},\boldsymbol{\sigma};\mathbf{f})$ is convex, but the complementarity term is not. However the whole functional $\mathcal{G}(\mathbf{u},\boldsymbol{\sigma},\mathbf{f},g)$ is strongly convex. Due to (5) and to the fact that, for $0 \leq t \leq 1$, $t(t-1) < 0$:

$$
\begin{aligned}
\mathcal{J}(t\mathbf{u}+(1-t)\mathbf{v}, t\boldsymbol{\sigma}+(1-t)\boldsymbol{\tau};\mathbf{f},g) &= t\mathcal{J}(\mathbf{u},\boldsymbol{\sigma};\mathbf{f},g) + (1-t)\mathcal{J}(\mathbf{v},\boldsymbol{\tau};\mathbf{f},g) + t(t-1)\mathcal{J}(\mathbf{u}-\mathbf{v},\boldsymbol{\sigma}-\boldsymbol{\tau};0,0) \\
&\leq t\mathcal{J}(\mathbf{u},\boldsymbol{\sigma};\mathbf{f},g) + (1-t)\mathcal{J}(\mathbf{v},\boldsymbol{\tau};\mathbf{f},g) + t(t-1)C_1 M(\mathbf{u}-\mathbf{v},\boldsymbol{\sigma}-\boldsymbol{\tau}) \\
&\leq t\mathcal{J}(\mathbf{u},\boldsymbol{\sigma};\mathbf{f},g) + (1-t)\mathcal{J}(\mathbf{v},\boldsymbol{\tau};\mathbf{f},g)
\end{aligned}
$$

where the last inequality holds due to the previous result. ■

Corollary 3.2.1. *For constants satisfying (10), the augmented LS functional is coercive.*

Proof. Consider the inequality from the previous lemma. It is known that, $\forall \boldsymbol{\sigma},\boldsymbol{\tau},\mathbf{u},\mathbf{v}$ in the adimissible set, $\mathcal{J}(t\mathbf{u}+(1-t)\mathbf{v}, t\boldsymbol{\sigma}+(1-t)\boldsymbol{\tau};\mathbf{f},g) \geq 0$. Therefore it holds:

$$
0 \leq t\mathcal{J}(\mathbf{u},\boldsymbol{\sigma};\mathbf{f},g) + (1-t)\mathcal{J}(\mathbf{v},\boldsymbol{\tau};\mathbf{f},g) + t(t-1)C_1 M(\mathbf{u}-\mathbf{v},\boldsymbol{\sigma}-\boldsymbol{\tau})
$$

Then fix $t \in (0,1)$, choose $\mathbf{v}$, $\boldsymbol{\tau}$ as the minimizer of the problem, so that $\mathcal{J}(\mathbf{v},\boldsymbol{\tau},\mathbf{f},g) = 0$. We get:

$$
\begin{aligned}
\frac{1}{C_1(1-t)}\mathcal{J}(\mathbf{u},\boldsymbol{\sigma},\mathbf{f},g) \geq & M(\mathbf{u}-\mathbf{v},\boldsymbol{\sigma}-\boldsymbol{\tau}) \\
= & \|\boldsymbol{\varepsilon}(\mathbf{u})\|_{L^2}^2 + \|\boldsymbol{\varepsilon}(\mathbf{v})\|_{L^2}^2 - 2\|\boldsymbol{\varepsilon}(\mathbf{u})\|_{L^2}\|\boldsymbol{\varepsilon}(\mathbf{v})\|_{L^2} + \|\boldsymbol{\tau}\|_{H_{div}}^2 + \|\boldsymbol{\sigma}\|_{H_{div}}^2 - 2\|\boldsymbol{\tau}\|_{H_{div}}\|\boldsymbol{\sigma}\|_{H_{div}} \\
= & M(\mathbf{v},\boldsymbol{\tau}) + M(\mathbf{u},\boldsymbol{\sigma}) - 2\|\boldsymbol{\varepsilon}(\mathbf{u})\|_{L^2}\|\boldsymbol{\varepsilon}(\mathbf{v})\|_{L^2} - 2\|\boldsymbol{\tau}\|_{H_{div}}\|\boldsymbol{\sigma}\|_{H_{div}} \to \infty
\end{aligned}
$$

Here $M(\mathbf{u},\boldsymbol{\sigma})$, $\|\boldsymbol{\varepsilon}(\mathbf{u})\|_{L^2}$, $\|\boldsymbol{\sigma}\|_{H_{div}}$ are constants because $(\mathbf{u},\boldsymbol{\sigma})$ is fixed. Now let $(\mathbf{v},\boldsymbol{\tau})$ be a sequence such that $M(\mathbf{v},\boldsymbol{\tau}) \to \infty$. Then the norm terms inside $M(\mathbf{v},\boldsymbol{\tau})$ are a quadratic form which grows faster than all the other addenda. Therefore coercivity follows. ■

Lemma 3.3. *For constants satisfying (10), it exists a unique minimizer* $(\boldsymbol{u}, \boldsymbol{\sigma}) \in K$ *of the augmented LS functional* $\mathcal{J}(\boldsymbol{u}, \boldsymbol{\sigma}; \boldsymbol{f}, g)$.

Proof. The proof follows from strong convexity, which implies strict convexity and coercivity, and from continuity of the functional, which implies the lower semicontinuity (see [14], chapter II, proposition 1.2) . ■

4 Monotone Multilevel

Using a direct solver for a large sparse system can be very demanding. Therefore iterative solvers are necessary. Nevertheless the rate of convergence of standard projected Gauß-Seidel deteriorates by reducing the meshwidth. Furthermore the behaviour gets worse with increasing the condition number. The FOSLS system gives rise to normal equations, i.e. a symmetric positive linear system, whose condition number can, unfortunately, be the square of the one of the original problem. All these reasons suggest to adopt a multilevel method. In particular, due to the local non-linearities and the convexity of the LS functional, we opt for a monotone multilevel. In this section we introduce a hierarchy of nested subspaces for displacements and stresses, together with the corresponding interpolation operators. Indeed these ones are main ingredients for a multilevel method. Moreover, decoupling normal and tangential components for the degrees of freedom on Γ_C, a proper basis transformation from the canonical coordinate system to the normal tangential coordinate system is thereafter exploited. All the relative quantities will be then represented in this new setting.

4.1 Discretization

Let $\mathcal{T}_1$ be a partition of Ω into finite elements τ (triangles in 2D or tetrahedra in 3D), with meshwidth parameter $h_1 = \max_{\tau \in \mathcal{T}_1} \operatorname{diam}(\tau)$ and $\Gamma_{C,1} = \mathcal{T}_1|_{\Gamma_C}$. Then recursively, for $j = 2, ..., J$, define $\mathcal{T}_j$, with the corresponding h_j and $\Gamma_{C,j}$, as the uniform refinement of $\mathcal{T}_{j-1}$. We also denote by $\mathcal{N}_j$, $\mathcal{E}_j$, $\mathcal{F}_j$ the sets of vertices, edges and faces of the mesh $\mathcal{T}_j$, and we set $N_j = |\mathcal{N}_j|$, $E_j = |\mathcal{E}_j|$, $F_j = |\mathcal{F}_j|$.
For the sake of simplicity, we also identify each entity, such as vertices, edges, faces and elements, with the corresponding points and subsets of points of $\mathbb{R}^1$, $\mathbb{R}^{d-1}$ and $\mathbb{R}^d$. This implies that we can also state if an entity belongs or not to another one. For example, whenever we say that a vertex ν belongs to a face ϕ, we mean that the point related to the vertex belongs to the set of points contained by the face itself, i.e. $\nu \in \phi$. Likewise an edge ϵ belongs to a face ϕ if all the points corresponding to it are contained in the set of points identified by the face, i.e. $\epsilon \in \phi$.
For k, $j = 1, ...J,$, we also define the following sets:

$$\begin{aligned} \mathcal{F}_k(\nu_j) &= \{\phi \in \mathcal{F}_k \mid \nu \in \phi, \nu \in \mathcal{N}_j \} \\ &= \text{set of all faces on level k to which the vertex } \nu \text{ on level j belongs} \end{aligned} \tag{11}$$

$$\begin{aligned} \mathcal{E}_k(\nu_j) &= \{\phi \in \mathcal{F}_k \mid \nu \in \phi, \nu \in \mathcal{N}_j \} \\ &= \text{set of all edges on level k to which the vertex } \nu \text{ on level j belongs} \end{aligned} \tag{12}$$

Moreover we can set the relationship, due to uniform refinement, from a father face to its sons, for $k = 1, ..., J-1$

$$\begin{aligned} \text{Sons}(\phi_k) &= \{\psi \in \mathcal{F}_{k+1} \mid \psi \in \phi, \phi \in \mathcal{F}_k\} \\ &= \text{set of all faces on level k+1 belonging to the face } \phi \text{ on level k} \end{aligned} \tag{13}$$

and from the son to the father, for $k = 1, ..., J-1$:

$$\begin{aligned} \text{Father}(\phi_{k+1}) &= \{\psi \in \mathcal{F}_k \mid \phi \in \psi, \phi \in \mathcal{F}_{k+1}\} \\ &= \text{face on level k containing the face } \phi \text{ on level k+1} \end{aligned} \tag{14}$$

Now let $P^1(\mathcal{T}_j)$ be the space of continuous piecewise linear functions on $\mathcal{T}_j$ with basis functions λ_{j,ν_p} such that:

$$\lambda_{j,\nu_p}(\nu_q) = \delta_{p,q} \qquad \forall \nu_q, \nu_p \in \mathcal{N}_j$$

and $\mathrm{RT}_0(\mathcal{T}_j)$ be the lowest order Raviart-Thomas space defined on $\mathcal{T}_j$ whose standard basis functions λ_{j,ϕ_p} must satisfy

$$\int_{\phi_q} \lambda_{j,\phi_p} \cdot \mathbf{n}_{\phi_q} = \delta_{p,q} \qquad \forall \phi_q, \phi_p \in \mathcal{F}_j$$

where $\mathbf{n}_{\phi_q}$ is the normal related to the face ϕ_q. The interpolation operators for nested meshes from level j to level $j+1$ are defined as follows:

$$\begin{aligned} &P_j^{j+1} : P^1(\mathcal{T}_j) \to P^1(\mathcal{T}_{j+1}) \qquad (P_j^{j+1}u - u)|_{\nu_{j+1}} = 0 \qquad \forall \nu_{j+1} \in \mathcal{N}_{j+1},\ \forall u \in P^1(\mathcal{T}_j) \\ &\Pi_j^{j+1} : \mathrm{RT}_0(\mathcal{T}_j) \to \mathrm{RT}_0(\mathcal{T}_{j+1}) \qquad \int_{\phi_{j+1}} (\Pi_j^{j+1}\mathbf{t} - \mathbf{t})\mathbf{n}_{j+1} ds = 0 \qquad \forall \phi_{j+1} \in \mathcal{F}_{j+1},\ \forall \mathbf{t} \in \mathrm{RT}_0(\mathcal{T}_j) \end{aligned} \tag{15}$$

Let $\mathbf{E}_k \in \mathbb{R}^d$, for $k = 1, .., d$, be the Cartesian unit vectors. For $j = 1, ..., J$ we also define the following finite element spaces:

$U_j = \left[P^1(\mathcal{T}_j)\right]^d$ with basis functions $\tilde{\boldsymbol{\lambda}}_{U_j,\nu}$, $\nu \in \mathcal{N}_j$, whose k-th component is $\left[\boldsymbol{\lambda}_{U_j,\nu}\right]_k = \lambda_{j,\nu}\mathbf{E}_k$

$\Sigma_j = [\mathrm{RT}_0(\mathcal{T}_j)]^d$ with basis functions $\tilde{\boldsymbol{\lambda}}_{\Sigma_j,\phi}$, $\phi \in \mathcal{F}_j$, whose k-th component is $\left[\boldsymbol{\lambda}_{\Sigma_j,\phi}\right]_k = \lambda_{j,\phi}\mathbf{E}_k$

$X_j = U_j \times \Sigma_j$ with basis functions $\left(\tilde{\boldsymbol{\lambda}}_{U_j,\nu}, \mathbf{0}\right)$, for $\nu \in \mathcal{N}_j$, and $\left(\mathbf{0}, \tilde{\boldsymbol{\lambda}}_{\Sigma_j,\phi}\right)$, for $\phi \in \mathcal{F}_j$

We will denote the set of basis functions of U_j, Σ_j, X_j respectively by Λ_{U_j}, Λ_{Σ_j}, Λ_{X_j}. Furthermore we define the corresponding interpolation operators componentwise using (15):

$$\mathbf{P}_j^{j+1} = \left[P_j^{j+1}\right]^d : \left[P^1(\mathcal{T}_j)\right]^d \to \left[P^1(\mathcal{T}_{j+1})\right]^d \qquad \boldsymbol{\Pi}_j^{j+1} = \left[\Pi_j^{j+1}\right]^d : [\mathrm{RT}_0(\mathcal{T}_j)]^d \to [\mathrm{RT}_0(\mathcal{T}_{j+1})]^d \tag{16}$$

Moreover, for the approximation of the trace spaces $\left[H^{1/2}(\Gamma_C)\right]^d$ and $\left[H^{-1/2}(\Gamma_C)\right]^d$ (for a precise definition of these spaces, we refer the reader to [18]), we use the trace spaces of the above finite element spaces:

$$U_{j,n} = \text{span}\left\{\lambda_{U_j,\nu,\text{n}} = \boldsymbol{\lambda}_{U_j,\nu} \cdot \mathbf{n}_\nu|_{\Gamma_C} \;\middle|\; \nu \in \mathcal{N}_j \cap \Gamma_C,\ \boldsymbol{\lambda}_{U_j,\nu} \in \Lambda_{U_j}\right\}$$
$$\Sigma_{j,n} = \text{span}\left\{\lambda_{\Sigma_j,\phi,\text{n}} = \boldsymbol{\lambda}_{\Sigma_j,\phi} \cdot \mathbf{n}_\phi|_{\Gamma_C} \;\middle|\; \phi \in \mathcal{F}_j \cap \Gamma_C,\ \boldsymbol{\lambda}_{\Sigma_j,\phi} \in \Lambda_{\Sigma_j}\right\}$$

The corresponding sets of basis functions will be denoted by $\Lambda_{U_j,\text{nt}}$ and $\Lambda_{\Sigma_j,\text{nt}}$. Also for these spaces, we can define interpolation operators between nested meshes:

$$P_{j,n}^{j+1} : U_{j,n} \to U_{j+1,n} \qquad\qquad \Pi_{j,n}^{j+1} : \Sigma_{j,n} \to \Sigma_{j+1,n} \tag{17}$$

Furthermore we denote the convex set of admissible displacements and stresses as:

$$K_J = \left\{\mathbf{x}_J = (\mathbf{u}_J, \boldsymbol{\sigma}_J) \in X_J : \quad \mathbf{u}_J|_{\Gamma_D} = \mathbf{u}_J^D,\ \boldsymbol{\sigma}_J|_{\Gamma_N} = \mathbf{t}_J^N,\ \mathbf{u}_J \cdot \mathbf{n}_J|_{\Gamma_C} \le g_J,\ \mathbf{n}^T(\boldsymbol{\sigma}_J\mathbf{n}) \le 0,\ \mathbf{t}_J^T(\boldsymbol{\sigma}\mathbf{n}_J) = 0\right\}$$

where $\mathbf{u}_J^D$, $\mathbf{t}_J^N$, $\mathbf{n}_J$, g_J, $\mathbf{f}_J$ are elements of the respective finite element spaces. The discrete minimization problem is then: find $(\mathbf{u}_J, \boldsymbol{\sigma}_J) \in K_J$ such that:

$$\mathcal{J}_J(\mathbf{u}_J, \boldsymbol{\sigma}_J; \mathbf{f}_J, g_J) \le \mathcal{J}_J(\mathbf{v}_J, \boldsymbol{\tau}_J; \mathbf{f}_J, g_J) \quad \forall\, (\mathbf{v}_J, \boldsymbol{\tau}_J) \in K_J \tag{18}$$

We note that, in general $K_J \not\subseteq K$. Nevertheless for shape regular tessellations $\mathcal{T}_J$, the approximate solution of the discretized problem converges to the solution of the continuum problem, as the meshwidth h_J tends to zero. For details we refer to [13, 18].
Whenever it will be no cause of misunderstanding, the subscript J will be omitted from the functional and the unknowns and, with an abuse of notation, we will write $\mathcal{J}(\mathbf{x}_J)$ instead of $\mathcal{J}(\mathbf{u}_J, \boldsymbol{\sigma}_J; \mathbf{f}_J, g_J)$.

4.2 Monotone multilevel method

The standard projected Gauß-Seidel or coordinate descent method successively minimizes the functional $\mathcal{J}$ in the directions $\lambda_J \in \Lambda_{X_J}$. However, for the ill-conditioned problems considered here, the rate of convergence of this method deteriorates for $h_J \to 0$. Such an inconvenience promoted the analysis of multilevel methods that involve coarse grid corrections as well. Specifically, the monotone multilevel idea is to extend the minimization process also to low frequency components of the spectrum. Therefore $\mathcal{J}$ is minimized with respect to all $\lambda_j \in \Lambda_{X_j}$, for $j = 1, ..., J$.
A prerequisite of multilevel methods is that eigenfunctions associated to small eigenvalues can be well represented on coarse meshes. This is well known for standard finite element discretizations, since the kernel of the gradient are the costant functions. However the kernel of the divergence operator is considerably larger. All divergence-free functions, also the ones with a large gradient, are contained in the kernel. This makes their representation on coarse meshes difficult or even impossible. To circumvent this drawback, different strategies have

been proposed [2, 3, 4, 16, 17]. Here we will focus on the one described in [2, 3, 4], but since (4) is a mixed formulation, an extension to primal and dual variables as in [26] is carried out.
Now let us fix the two levels j and k to be the same, i.e. $j = k$. For fixed vertex $\nu \in \mathcal{N}_j$ and abitrary faces $\phi \in \mathcal{F}_j$, we then define the patch associated to ν as the union of the vertex ν and the set $\mathcal{F}_j(\nu_j)$(compare with (11)), containing all the faces of the mesh $\mathcal{T}_j$ which share the fixed vertex $\nu \in \mathcal{N}_j$. We denote by $\Lambda_{j,\nu}$ the collection of basis functions in Λ_{U_j}, related to the vertex ν, and in Λ_{Σ_j}, related to faces of $\mathcal{F}_j(\nu_j)$. Therefore we can write:

$$\begin{aligned} &\Lambda_{j,\nu} = \left\{\boldsymbol{\lambda}_{U_j,\nu}\right\} \cup \left\{\boldsymbol{\lambda}_{\Sigma_j,\phi} \in \Lambda_{\Sigma_j} : \phi \in \mathcal{F}_j(\nu_j),\ \phi \in \mathcal{F}_j\right\} && j = 2, ..., J, \\ &\Lambda_1 = \{\boldsymbol{\lambda}_{U_1,\nu} \in \Lambda_{U_1},\ \boldsymbol{\lambda}_{\Sigma_1,\phi} \in \Lambda_{\Sigma_1} : \nu \in \mathcal{N}_1,\ \phi \in \mathcal{F}_1\} && j = 1 \end{aligned}$$

where the minimization problem is solved exactly on the coarse level $j = 1$.
Consequently $\mathcal{J}$ has to be minimized with respect to $\Lambda_{j,\nu}$, for $j = J, ..., 2$, $\nu = 1, ..., N_j$, and Λ_1. Since the functional is strongly convex and differentiable, the discrete minimization problem (18) can be reformulated as the variational inequality (4). For simplicity, we consider only one pre-smoothing step, i.e. N_j sub-steps on each level. Given an admissible starting iterate $\mathbf{x}_J^0$, let $\mathbf{x}_J^k \in K_J$ be the k-th iterate, for $k \in \mathbb{N}$. Then we define $\mathbf{x}_{J,0} = \mathbf{x}_J^k$ and $\mathbf{x}_{j,0} = \mathbf{x}_{j+1,N_{j+1}}$, for $j = J-1, ..., 1$. We compute a sequence of intermediate iterates $\mathbf{x}_{j,\nu} = \mathbf{x}_{j,\nu-1} + \mathbf{c}_{j,\nu}$ by solving:

$$\text{find } \mathbf{c}_{j,\nu} \in K_{j,\nu}^* : \quad \mathcal{J}(\mathbf{x}_{j,\nu-1} + \mathbf{c}_{j,\nu}) \leq \mathcal{J}(\mathbf{x}_{j,\nu} + \mathbf{y}) \quad \forall \mathbf{y} \in K_{j,\nu}^* \quad j = J, ..., 2, \quad \nu = 1, ..., N_j \tag{19}$$

$$\text{find } \mathbf{c}_1 \in K_1^* : \quad \mathcal{J}(\mathbf{x}_{2,N_2} + \mathbf{c}_1) \leq \mathcal{J}(\mathbf{x}_{2,N_2} + \mathbf{y}) \quad \forall \mathbf{y} \in K_1^* \quad j = 1 \tag{20}$$

where the local closed convex sets $K_{j,\nu}$ and K_1^* are defined as follows:

$$\begin{aligned} K_{j,\nu}^*(\mathbf{x}_{j,\nu-1}) &= \{\mathbf{y} \in \text{span}\{\Lambda_{j,\nu}\} : \quad \mathbf{y} + \mathbf{x}_{j,\nu-1} \in K_J\} \\ K_1^*(\mathbf{x}_{2,N_2}) &= \{\mathbf{y} \in \text{span}\{\Lambda_1\} : \quad \mathbf{y} + \mathbf{x}_{2,N_2} \in K_J\} \end{aligned} \tag{21}$$

In order to compute the solution of these local problems, a comparison with the constraints on the fine level is needed. However evaluating quantities which live on the finer meshes can lead to algorithms with suboptimal complexity. To recover an optimal complexity, only an approximate solution, instead of the exact one, can be taken into consideration for coarser levels. To this aim, we define approximate convex sets K_j and, thus, proper coarse constraints which will depend on the current iterate and on the corrections on the higher levels. Two specific non-linear projections, one for the normal displacement and the other for the pressure, will be later investigated [20, 21, 25].

Remark. *In minimizing the functional $\mathcal{J}$ along the directions $\Lambda_{j,\nu}$, the order has been chosen in this way: $j = J, ..., 1$ and, for a fixed level j, from $\nu = 1$ to $\nu = N_j$. This scheme corresponds only to a pre-smoothing plus an active set method on the coarsest level. Anyhow,*

after this pre-smoothing, the order can be inverted again, i.e. $j = 2, ..., J$, $\nu = N_j, ..., 1$, *so that a post-smoothing with an overall symmetric cycle is recovered. Similarly more than one smoothing step can be performed. However, for simplicity of notation, only a pre-smoothing is presented in the analysis.*

4.3 Change of coordinates

In order to properly describe contact conditions also on coarser levels, it is wise to locally change the coordinate system of the contact boundary Γ_C. In this way, the scalar constraints have to be checked directly on the normal components and not on some linear combinations of the unknown. Let $\nu \in \mathcal{N}_j \cap \Gamma_{C,j}$ and $\mathbf{n}_\nu$ be the obstacle normal in ν. Then consider the vector $\mathbf{U}_\nu \in \mathbb{R}^d$ that contains the degrees of freedom of the displacement associated to ν. Define the Householder transformation $\mathbf{H}_\nu$ relative to the ouward normal $\mathbf{n}_\nu$ and the local displacement in the normal tangential coordinate system $\mathbf{U}_{\nu,nt}$ (the first coordinate is the normal one) respectively as:

$$\mathbf{H}_\nu = \mathbf{I} - 2\,\mathbf{n}_\nu^T \mathbf{n}_\nu \qquad\qquad \mathbf{U}_{\nu,nt} = \mathbf{H}_\nu \mathbf{U}_\nu$$

A similar argument has to be applied to the stress components. For each face $\phi \in \Gamma_{C,j}$, consider the normal to the face $\mathbf{n}_\phi$ and the stress $\boldsymbol{\sigma}$. We can express the vector unknown $\boldsymbol{\Sigma}_\phi$, associated to the face ϕ, in terms of the normal and tangent forces $\boldsymbol{\Sigma}_{\phi,nt}$. It is not convenient to use direclty the HouseHolder transformation $\mathbf{H}_\phi$ relative to the face normal $\mathbf{n}_\phi$, because we have no control on the sign of $\left(\boldsymbol{\lambda}_{\Sigma_j,\phi} \cdot \mathbf{n}_\phi\right)$. In its place, it is preferrable the transformation $\mathbf{Q}_\phi$:

$$\boldsymbol{\sigma}\mathbf{n}_\phi = \left(\boldsymbol{\lambda}_{\Sigma_j,\phi} \cdot \mathbf{n}_\phi\right) \boldsymbol{\Sigma}_\phi = \mathbf{H}_\phi \boldsymbol{\Sigma}_{\phi,nt} \quad \iff \quad \boldsymbol{\Sigma}_\phi = \frac{1}{\left(\boldsymbol{\lambda}_{\Sigma_j,\phi} \cdot \mathbf{n}_\phi\right)} \mathbf{H}_\phi \boldsymbol{\Sigma}_{\phi,nt} = \mathbf{Q}_\phi \boldsymbol{\Sigma}_{\phi,nt}$$

In this way the first component of $\mathbf{U}_{\nu,nt}/\boldsymbol{\Sigma}_{\phi,nt}$ is actually positive in the direction of the normal $\mathbf{n}_\nu/\mathbf{n}_\phi$. Furthermore the constraints can be direclty compared with the coefficients of the functions in the new basis. Computationally speaking, this is a simplification that does not have to be underestimated.
All the degrees of freedom on the contact boundary will be treated as normal or tangent. The relative change of coordinates is equivalent to a change of basis, so that all the previous definitions of $\Lambda_{U_j,\nu}$, $\Lambda_{\Sigma_j,\nu}$, $\Lambda_{j,\nu}$ have to be consequently adapted to $\Lambda_{U_j,nt}$ and $\Lambda_{\Sigma_j,nt}$:

$$\Lambda_{U_j,nt} = \left\{\boldsymbol{\lambda}_{U_j,\nu,nt}, \quad \nu \in \mathcal{N}_j\right\} \qquad \boldsymbol{\lambda}_{U_j,\nu,nt} = \begin{cases} \boldsymbol{\lambda}_{U_j,\nu}\mathbf{H}_\nu & \nu \in \Gamma_{C,j} \\ \boldsymbol{\lambda}_{U_j,\nu} & \nu \notin \Gamma_{C,j} \end{cases} \qquad j = 1, ..., J,\ \nu \in \mathcal{N}_j$$

$$\Lambda_{\Sigma_j,nt} = \left\{\boldsymbol{\lambda}_{\Sigma_j,\phi,nt}, \quad \phi \in \mathcal{F}_j\right\} \qquad \boldsymbol{\lambda}_{\Sigma_j,\phi,nt} = \begin{cases} \boldsymbol{\lambda}_{\Sigma_j,\phi}\mathbf{Q}_\phi & \phi \in \Gamma_{C,j} \\ \boldsymbol{\lambda}_{\Sigma_j,\phi} & \phi \notin \Gamma_{C,j} \end{cases} \qquad j = 1, ..., J,\ \nu \in \mathcal{N}_j$$

It is important to notice that the change of basis has a direct impact on the system and on the interpolation operators. Let $\mathbf{H}$ be the global Householder matrix, which collects all the local matrices $\mathbf{H}_\nu$ and $\mathbf{Q}_\phi$, while it is the identity on interior degrees of freedom. This operator can be used to redefine, once and for all, *all* the quantities in the normal-tangential coordinate system. However, for the sake of simplicity of notation, from now on we will omit the relative subscript $_{nt}$ and we will denote the normal or tangent components by the notation: $[\cdot]_i$, for $i = n, t$.

5 Non-linear projection operators and coarse constraints

To obtain optimal complexity, all the quantities of a given level j should have a size that is proportional to the level itself. This means that no comparison with entities belonging to finer levels should be considered. In particular, instead of the constraints on level J, new coarse constraints and, consequently, proper convex sets K_j should be introduced. We define the convex sets on the fine level K_J and on the coarser level K_j, for $j = J-1, ..., 1$, in the following way:

$$K_J = \left\{\mathbf{x}_J = (\mathbf{u}_J, \boldsymbol{\sigma}_J) \in X_J : \mathbf{u}_J|_{\Gamma_D} = \mathbf{u}_J^D,\ \boldsymbol{\sigma}_J|_{\Gamma_N} = \mathbf{t}_J^N,\ \mathbf{u}_J \cdot \mathbf{n}_J|_{\Gamma_C} \leq g_J,\ \mathbf{n}^T(\boldsymbol{\sigma}_J\mathbf{n}) \leq 0,\ \mathbf{t}_J^T(\boldsymbol{\sigma}\mathbf{n}_J) = 0\right\} \tag{22}$$

$$K_j = \left\{\mathbf{x}_j = (\mathbf{u}_j, \boldsymbol{\sigma}_j) \in X_j : \mathbf{u}_j|_{\Gamma_D} = \mathbf{0},\ \boldsymbol{\sigma}_j|_{\Gamma_N} = \mathbf{0},\ \mathbf{u}_J \cdot \mathbf{n}_j|_{\Gamma_C} \leq g_{j,u_n},\ \mathbf{n}^T(\boldsymbol{\sigma}_j\mathbf{n}) \leq g_{j,\sigma_n},\ \mathbf{t}_J^T(\boldsymbol{\sigma}\mathbf{n}_J) = 0\right\} \tag{23}$$

Given an initial guess $\mathbf{x}_J^0$ belonging to the admissible set, let $\mathbf{c}_{j,\nu} = (\mathbf{u}_{j,\nu}, \boldsymbol{\sigma}_{j,\nu})$ be the correction at level j on the patch identified by ν. Furthermore let $\mathbf{c}_{J,0} = \mathbf{x}_J^k$, $\mathbf{c}_{j,0} = \mathbf{0}$ for $j = J-1, ..., 1$ and $\mathbf{w}_{j,\nu} = \sum_{\mu=0}^{\nu} \mathbf{c}_{j,\mu}$ be respectively the current iterate, the first corrections on level j and the sum of all the corrections on the same level j until the vertex ν. Unlike (19), we solve the following approximate local problem: successively find $\mathbf{c}_{j,\nu} \in K_{j,\nu}(\mathbf{w}_{j,\nu-1})$ and $\mathbf{c}_1 \in K_1$ such that:

$$\begin{aligned}
&\bullet\ j = J, ..., 2,\ \ \nu = 1, ..., N_j : \\
&\qquad \mathcal{J}(\mathbf{w}_{j,\nu-1} + \mathbf{c}_{j,\nu}) \leq \mathcal{J}(\mathbf{w}_{j,\nu-1} + \mathbf{y}) \quad \forall\, \mathbf{y} \in K_{j,\nu}(\mathbf{w}_{j,\nu-1}) = \{\mathbf{y} \in \mathrm{span}\{\Lambda_{j,\nu}\} :\ \mathbf{y} + \mathbf{w}_{j,\nu-1} \in K_j\} \\
&\bullet\ j = 1 : \\
&\qquad \mathcal{J}(\mathbf{c}_1) \leq \mathcal{J}(\mathbf{y}) \qquad\qquad \forall\, \mathbf{y} \in K_1
\end{aligned} \tag{24}$$

where, as opposed to (21), in $K_{j,\nu}(\mathbf{w}_{j,\nu-1})$ we consider K_j instead of K_J. It is evident that, if $K_j \subset K_{j+1}$ for $j = 1, ..., J-1$, then $K_{j,\nu} \subset K_{j,\nu}^*$, which also implies that all the intermediate approximations of the solution belong to K_J. Thus we must choose the coarse constraints function g_{j,u_n} and g_{j,σ_n} so that $K_j \subset K_{j+1}$. Of course g_{j,u_n} and g_{j,σ_n} will respectively depend on g_{j+1,u_n} and g_{j+1,σ_n} and, to this aim, specific projection operators need to be examined.
We set $H = j$, $h = j+1$. Then $\mathcal{T}_H = \mathcal{T}_j$ is a mesh at level j and $\mathcal{T}_h = \mathcal{T}_{j+1}$ is its uniform refinement. Let $\varepsilon \in \mathcal{E}_H \cap \Gamma_{C,H}$ be a coarse edge which contains the two coarse vertices $\nu_{\varepsilon,1}$,

$\nu_{\varepsilon,2} \in \mathcal{N}_H$, on its ends, and a fine midpoint $\nu_h \in \mathcal{N}_h$. Let $v_h \in U_{h,n}$ be a linear function defined on $\Gamma_{C,h}$. Its non-linear projection $v_H = I_h^H(v_h) \in U_{H,n}$ must fulfill $v_H \leq v_h$ and, consequently, $P_{H,n}^h v_H \leq v_h$, where $P_{H,n}^h$ is defined in (17) (remind that now everything is expressed in the new coordinate system). This is equivalent to require the following:

$$\begin{aligned} & v_H(\nu_{\varepsilon,1}) \leq v_h(\nu_{\varepsilon,1}) \\ & v_H(\nu_{\varepsilon,2}) \leq v_h(\nu_{\varepsilon,2}) \\ & \frac{1}{2}(v_H(\nu_{\varepsilon,1}) + v_H(\nu_{\varepsilon,2})) \leq v_h(\nu_h) \end{aligned} \qquad \forall \varepsilon \in \mathcal{E}_H \cap \Gamma_{C,H} \tag{25}$$

It is easy to see that, on a given ε, the following values satisfy the three conditions above:

$$a) \quad \begin{cases} \tilde{v}_H(\nu_{\varepsilon,1}, \varepsilon) = \min(v_h(\nu_{\varepsilon,1}), \max(v_h(\nu_h), 2v_h(\nu_h) - v_h(\nu_{\varepsilon,2}))) \\ \tilde{v}_H(\nu_{\varepsilon,2}, \varepsilon) = \min(v_h(\nu_{\varepsilon,2}), \max(v_h(\nu_h), 2v_h(\nu_h) - v_h(\nu_{\varepsilon,1}))) \end{cases} \tag{26}$$

$$b) \quad \begin{cases} \tilde{v}_H(\nu_{\varepsilon,1}, \varepsilon) = \min(v_h(\nu_{\varepsilon,1}), v_h(\nu_h)) \\ \tilde{v}_H(\nu_{\varepsilon,2}, \varepsilon) = \min(v_h(\nu_{\varepsilon,2}), v_h(\nu_h)) \end{cases} \tag{27}$$

$$c) \quad \begin{cases} \tilde{v}_H(\nu_{\varepsilon,1}, \varepsilon) = \min(v_h(\nu_{\varepsilon,1}), v_h(\nu_h), v_h(\nu_{\varepsilon,2})) \\ \tilde{v}_H(\nu_{\varepsilon,2}, \varepsilon) = \min(v_h(\nu_{\varepsilon,1}), v_h(\nu_h), v_h(\nu_{\varepsilon,2})) \end{cases} \tag{28}$$

Anyhow, all the edges to which a coarse vertex belongs need to be considered. Therefore the effect of the non linear interpolation I_h^H can be summarized in this way:

$$v_H = I_{h,u_n}^H v_h = \sum_{\nu_H \in \mathcal{N}_H \cap \Gamma_{C,H}} [\lambda_{U_H,\nu_H}]_n \; v_H(\nu_H) \qquad \text{with} \qquad v_H(\nu_H) = \min_{\varepsilon \in \mathcal{E}_H(\nu_H)} \tilde{v}_H(\nu_H, \varepsilon) \tag{29}$$

Now consider a coarse face $\phi \in \mathcal{F}_H \cap \Gamma_{C,H}$ and its sons fine faces, i.e. $\text{Sons}(\phi)$ (compare with (13)). Then consider $s_h \in \Sigma_{h,n}$, a piecewise constant function on $\Gamma_{C,h}$. We want to define its non-linear projection $s_H = I_{h,\sigma_n}^H s_h \in \Sigma_{H,n}$ so that $s_H \leq s_h$ and $\Pi_{H,n}^h s_H \leq s_h$, where $\Pi_{H,n}^h$ is defined in (17). It suffices that:

$$s_H(\phi) \leq s_h(\phi_h) \quad \forall \phi_h \in \text{Sons}(\phi)$$

Thus:

$$s_H = I_{h,\sigma_n}^H s_h = \sum_{\phi \in \mathcal{F}_H \cap \Gamma_{C,H}} [\lambda_{\Sigma_H,H}]_n \; s_H(\phi) \qquad \text{with} \qquad s_H(\phi) = \min_{\phi_h \in \text{Sons}(\phi)} s_h(\phi_h) \tag{30}$$

Once the non-linear projections for both spaces have been introduced, let $g_J \in U_{J,n}$ and $0 \in \Sigma_{J,n}$ be the fine constraints of the problem. Then, for each level $j = 1, ..., J$, we define

coarse constraints $g_{j,u_n} \in U_{j,n}$, for the normal displacement corrections (recall that $\mathbf{u}_{j+1,\nu}$ and $\boldsymbol{\sigma}_{j+1,\nu}$ are corrections):

$$\begin{cases} g_{J,u_n} = g & j = J \\ g_{j,u_n} = I^j_{j+1,u_n}\left(g_{j+1,u_n} - \sum_{\nu=1}^{N_{j+1}} \left[\mathbf{u}_{j+1,\nu}|_{\Gamma_C}\right]_n\right) & j = J-1, ..., 1 \end{cases} \tag{31}$$

and $g_{j,\sigma_n} \in \Sigma_{j,n}$, for the pressure corrections:

$$\begin{cases} g_{J,\sigma_n} = 0 & j = J \\ g_{j,\sigma_n} = I^j_{j+1,\sigma_n}\left(g_{j+1,\sigma_n} - \sum_{\nu=1}^{N_{j+1}} \left[\boldsymbol{\sigma}_{j+1,\nu}|_{\Gamma_C}\right]_n\right) & j = J-1, ..., 1 \end{cases} \tag{32}$$

By exploiting (29), (30), (31), (32) and the definitions of the interpolation operators (16), it follows $K_j \subset K_{j+1}$ for $j = 1, ..., J-1$:

$$\begin{aligned} \sum_{\nu=1}^{N_j} \left[\mathbf{u}_{j,\nu}|_{\Gamma_C}\right]_n \leq g_{j,u_n} \quad &\Rightarrow \quad P^{j+1}_{j,n}\left(\sum_{\nu=1}^{N_j} \left[\mathbf{u}_{j,\nu}|_{\Gamma_C}\right]_n\right) \leq g_{j+1,u_n} - \sum_{\nu=1}^{N_{j+1}} \left[\mathbf{u}_{j+1,\nu}|_{\Gamma_C}\right]_n \\ \sum_{\nu=1}^{N_j} \left[\boldsymbol{\sigma}_{j,\nu}|_{\Gamma_C}\right]_n \leq g_{j,\sigma_n} \quad &\Rightarrow \quad \Pi^{j+1}_{j,n}\left(\sum_{\nu=1}^{N_j} \left[\boldsymbol{\sigma}_{j,\nu}|_{\Gamma_C}\right]_n\right) \leq g_{j+1,\sigma_n} - \sum_{\nu=1}^{N_{j+1}} \left[\boldsymbol{\sigma}_{j+1,\nu}|_{\Gamma_C}\right]_n \end{aligned}$$

Furthermore, by iterating the same argument for each level, it is clear that adding to the current iterate $\mathbf{x}^k$ all the corrections $\sum_{j=1}^{J}\sum_{\nu}^{N_j} \mathbf{c}_{j,\nu} \in K_J$, the resulting vector is still in the admissible set:

$$\begin{aligned} \sum_{j=1}^{J-1}\prod_{k=j}^{J-1} P^{k+1}_{k,n}\left(\sum_{\nu=1}^{N_k} \left[\mathbf{u}_{k,\nu}|_{\Gamma_C}\right]_n\right) + \left(\sum_{\nu=1}^{N_J} \left[\mathbf{u}_{J,\nu}|_{\Gamma_C}\right]_n\right) \leq g, \\ \sum_{j=1}^{J-1}\prod_{k=j}^{J-1} \Pi^{k+1}_{k,n}\left(\sum_{\nu=1}^{N_k} \left[\boldsymbol{\sigma}_{k,\nu}|_{\Gamma_C}\right]_n\right) + \left(\sum_{\nu=1}^{N_J} \left[\boldsymbol{\sigma}_{J,\nu}|_{\Gamma_C}\right]_n\right) \leq 0 \end{aligned}$$

6 Truncated Basis

We can define the set of active nodes and faces on the level j in the following way:

$$\begin{aligned} \mathcal{N}^{\bullet}_j &= \left\{ \nu \in \mathcal{N}_j \cap \Gamma_{C,j} : \quad g_{j,u_n}\big|_{\nu} = \sum_{\nu=1}^{N_j} \left[\mathbf{u}_{j,\nu}\big|_{\Gamma_C}\right]_n \right\} \\ \mathcal{F}^{\bullet}_j &= \left\{ \phi \in \mathcal{F}_j \cap \Gamma_{C,j} : \quad g_{j,\sigma_n}\big|_{\phi} = \sum_{\nu=1}^{N_j} \left[\boldsymbol{\sigma}_{j,\nu}\big|_{\Gamma_C}\right]_n \right\} \end{aligned} \tag{33}$$

By definition $g_{j,u_n}, g_{j,\sigma_n} \geq 0$. So it is clear that if at some level exists a $\nu_{j+1} \in \mathcal{N}_{j+1}^{\bullet}$ or a $\phi_{j+1} \in \mathcal{F}_{j+1}^{\bullet}$, the corresponding constraints on the successive coarser level j will be zero on all the nodes $\nu_j \in \varepsilon_{j+1}$ such that $\nu_{j+1} \in \varepsilon_{j+1}$ or on the face Father(ϕ_{j+1}). Consequently no positive coarse correction in the direction of the obstacle can be expected there. If also the correction on level j is zero on ν_j or ϕ_j, then $\nu_j \in \mathcal{N}_j^{\bullet}$ or a $\phi_j \in \mathcal{F}_j^{\bullet}$ and the previous argument can be repeated. By following this path of reasoning, it turns out that less and less coarse corrections which are positive in the normal direction can be picked. Since we are not able to properly improve the solution in the obstacle direction, a slow down in the convergence speed has to be expected. The truncated basis strategy, already proposed in [20], is the solution to this problem. The idea is to consider the sets of basis functions as dependent on the current intermediate iterate, by switching off the degrees of freedom $\nu_j \in \mathcal{N}_j^{\bullet}$ or a $\phi_j \in \mathcal{F}_j^{\bullet}$ for each level $j = J, ..., 1$. In this way, the correction coming from the lower level will be large enough to not slow down the convergence.
The truncated basis of level $j = J, ..., 1$, for $\nu \in \mathcal{N}_j$, $\phi \in \mathcal{F}_j$, is:

$$\left[\tilde{\boldsymbol{\lambda}}_{U_j,\nu}\right]_i = \begin{cases} \left[\boldsymbol{\lambda}_{U_j,\nu}\right]_i & \nu \in \mathcal{N}_j \setminus \mathcal{N}_j^{\bullet},\ i = n,t \\ 0 & \nu \in \mathcal{N}_j^{\bullet}, \quad i = n \\ \left[\boldsymbol{\lambda}_{U_j,\nu}\right]_i & \nu \in \mathcal{N}_j^{\bullet}, \quad i = t \end{cases} \qquad \left[\tilde{\boldsymbol{\lambda}}_{\Sigma_j,\phi}\right]_i = \begin{cases} \left[\boldsymbol{\lambda}_{\Sigma_j,\phi}\right]_i & \phi \in \mathcal{F}_j \setminus \mathcal{F}_j^{\bullet},\ i = n,t \\ 0 & \phi \in \mathcal{F}_j^{\bullet} \quad i = n \\ \left[\boldsymbol{\lambda}_{\Sigma_j,\phi}\right]_i & \phi \in \mathcal{F}_j^{\bullet}, \quad i = t \end{cases} \tag{34}$$

The truncated basis of the corresponding coarse subspace of level $j-1$ can be expressed as a linear combination of the truncated basis of level j. Then the corrections on level $j-1$ can be computed and new active degrees of freedom can be determined. Therefore the basis on a level j will strictly depend on the one of the immediately higher level. Since all $\tilde{\boldsymbol{\lambda}}_{U_j,\nu}$ and $\tilde{\boldsymbol{\lambda}}_{\Sigma_j,\phi}$ depend on the $\mathcal{N}_j^{\bullet}$ and $\mathcal{F}_j^{\bullet}$, which in turn depend on the current intermediate iterate on level j, i.e. $\mathbf{x}^k + \sum_{j=1}^{J}\sum_{\nu}^{N_j} \mathbf{c}_{j,\nu}$, the truncated basis will depend on it as well.
The truncation, that is simply a change of basis, affects all the quantities and all the transfer operators of each level. Particular care must be taken for the assembling of the interpolation operators, coarse matrices and vectors. Specifically the constraints g_{j,u_n}, g_{j,σ_n} can be defined in the usual way, except for the degrees of freedom $\nu_{j+1} \in \mathcal{N}_{j+1}^{\bullet}$ or $\phi_{j+1} \in \mathcal{F}_{j+1}^{\bullet}$. To this aim, before projecting onto the coarser level, we redefine:

$$g_{j+1,u_n}\big|_{\nu_{j+1}} - \sum_{\nu=1}^{N_{j+1}} \left[\mathbf{u}_{j+1,\nu}\big|_{\Gamma_C}\right]_n = +\infty, \qquad \nu_{j+1} \in \mathcal{N}_{j+1}^{\bullet} \tag{35}$$

$$g_{j+1,\sigma_n}\big|_{\phi_{j+1}} - \sum_{\nu=1}^{N_{j+1}} \left[\boldsymbol{\sigma}_{j+1,\nu_{j+1}}\big|_{\Gamma_C}\right]_n = +\infty \quad \phi_{j+1} \in \mathcal{F}_{j+1}^{\bullet} \tag{36}$$

so that all vertices and faces that fulfill equality constraints have no influence on coarser corrections.

7 Numerical Experiments

The definition of the augmented functional $\mathcal{J}$ in (1) is not unique and depends on the weights that are chosen for each term. One of these constants is arbitrary and can be fixed as the reference value, e.g. $C_{\text{const}} = 1$, while all the others must depend on this one. Experimentally a higher value for C_{eq} is necessary for capturing the stress. Anyhow, no matter which values are used for C_{const} and C_{eq}, the resulting linear system will be symmetric and positive definite. On the other hand the complementarity contribution is non negative if and only if it is evaluated on the convex set. Nevertheless, in the discrete form, such term does not correspond to a positive definite matrix. As a consequence, the matrix of the overall problem is for sure symmetric, but it can be positive or indefinite according to the weights C_{eq}, C_{const}, C_{compl}. In order to avoid indefinite problems, a C_{compl} which is not too large has to be considered (see 10). At the same time, it must not be too small, otherwise we would not be able to describe contact conditions. For FOSLS problems, a compromise is always required. A typical decision for the following tests can be C_{eq} =1e2, 1e3, C_{const} =1, C_{compl} =1e1, 1e2. For all the experiments here presented, the initial guess is computed as the solution of the problem on the coarsest mesh, then interpolated until the finest tassellation. This approach guarantees that for simulations with more levels, the initial guess is actually the same. For two levels, it also coincides with the nested iteration strategy.

Let $\Omega = [0,1] \times [0,1]$ be a square domain, with sides left, bottom, right, top. We enforce a displacement $\mathbf{u}|_{\text{top}} = (0, -0.01)$ and zero stresses on the left and right sides, $\boldsymbol{\sigma}\mathbf{n}|_{\text{left},right} = \mathbf{0}$. The bottom line is actually Γ_C. The domain lies on the straight rigid foundation, described by the gap function $g(x, y) = 0$ and by the obstacle normal $\mathbf{n}(x, y) = (0, 1)$. Thus, after the application of a uniform displacement on the top, the square will deform so that no penetration with the rigid obstacle occur.
The coarse mesh consists of only two elements. Then we uniformly refine this mesh until the level $J = 9$. We solve the problem by means of the monotone multilevel method. We use, for each level $j > 1$, 3 pre-smoothing and 3 post-smoothing, while, on the coarse level, we exploit the active set method. We study the convergence for the compressible and incompressible cases, i.e. $(\mu, \lambda) = (1, 1)$ and $(\mu, \lambda) = (1, \infty)$. As non-linear projection, we use the c) in (28). But, since the square is already in contact and the initial guess is computed as previously mentioned, after one smoothing step all the active degrees of freedom are detected. Therefore the problem reduces to a linear one.
We can see that the convergence, for more than six levels, is reached around 20 iterations for the compressible material and around 30 for the incompressible one, with a constant limit convergence rate which is respectively about 0.7 and 0.6. In the first situation, we can also see that the behaviour is non-linear at the beginning and only after a while the convergence rate becomes constant. For the incompressible material, on the other hand, the convergence rate is practically constant. Furthermore, in the limit case, it is smaller than the one for

$\lambda = 1$. This suggests that for incompressible materials, this method can be very attractive.

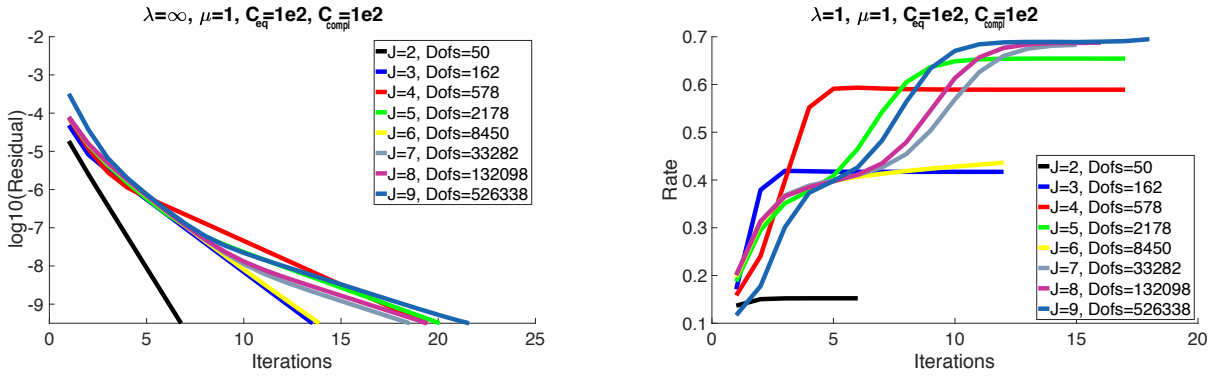

Figure 1: Square mesh. Compressible material.

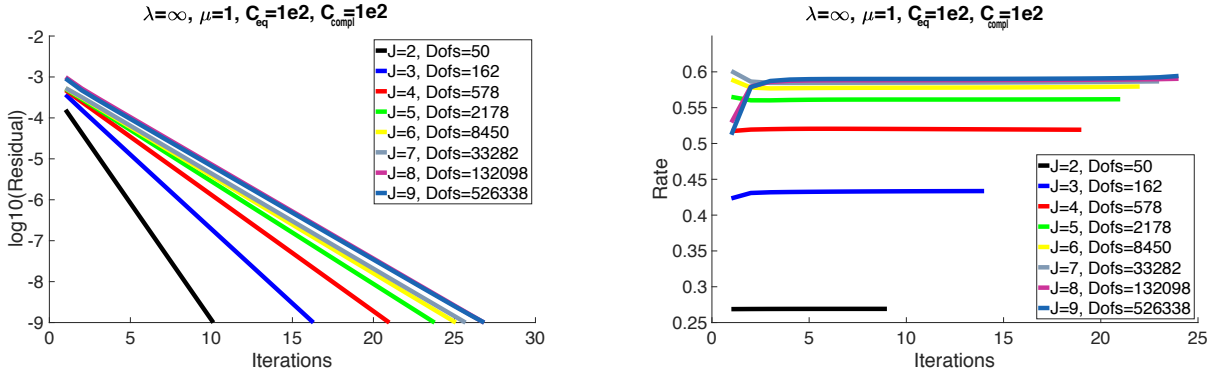

Figure 2: Square mesh. Incompressible material.

Now we consider the Hertz's problem for a semicircle of radius $r = 0.5$ and center $\mathbf{c} = (0, 1)$ which is pushed towards a rigid plane $f(x, y) = 0$ by a uniform displacement $\mathbf{u} = (0, -0.01)$ applied at the top. In this situation we just use a two level method. Indeed, for a circular mesh, non-nested semi-circular refinements would be optimal, but it is not an assumption of our framework. Therefore, given a semicircle coarse mesh, we just refine it one time. Altough the refinement is not optimal and the complementarity condition is just a penalty term, a two-level method still gives good results for the Signorini's problem. See picture 3).

We study the convergence for the compressible and incompressible cases, i.e. $(\mu, \lambda) = (1, 1)$ and $(\mu, \lambda) = (1, \infty)$. For each of these, we exploit the three kinds of projection operators a), b), c) in (26), (27), (28). In addition, we consider the case d) in which the coarse constraints are enforced equal to infinity. The number of smoothing-steps is 5, C_{eq} =1e2 and C_{compl} =1e1. In pictures 4), 5) and 6) we study the behaviour of a two level

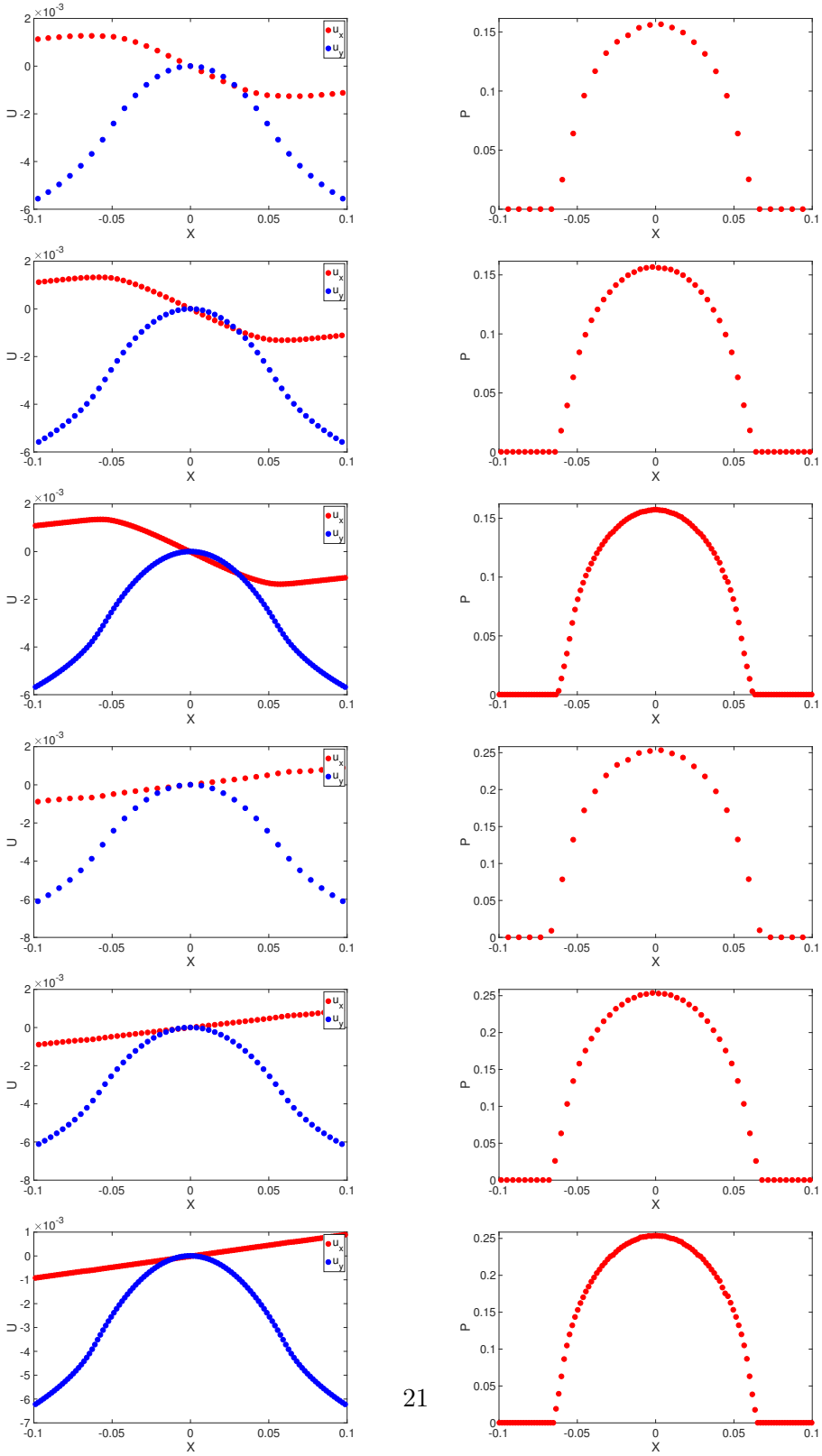

Figure 3: On the left, contact displacement components. On the right: the contact pressure. First three rows: $(\mu, \lambda) = (1, 1)$ for meshes with $h_{\max}/h_{\min} = 3.1688, 7.0567, 29.7936$. Last three rows: $(\mu, \lambda) = (1, \infty)$ for meshes with $h_{\max}/h_{\min} = 3.1688, 7.0567, 29.7936$.

method for three different meshes, whose ratio $h_{\max}/h_{\min} = 3.1688, 7.0567, 29.7936$, where $h_{\max} = \max_{\tau\in\mathcal{T}_1} \operatorname{diam}(\tau)$ and $h_{\min} = \min_{\tau\in\mathcal{T}_1} \operatorname{diam}(\tau)$. The less uniform the mesh and the more the contact boundary is refined.
The history of the sequence of iterations can be subdivided into three general main phases:

I a non linear phase in which the high frequencies components of the error are damped, with a non linearly increasing convergence rate; here the active set of the current iterate can (square example) or cannot (half-circle) coincide with the one of the solution;

II a non linear phase in which the active set of the current iterate does not coincide with the one of the solution, although the convergence rate is linear;

III a linear phase in which the active set of the current iterate coincides with the one of the solution (this condition is attained for sure for $k \to \infty$, as established in [20]);

In principle I), II) and III) should occur sequentially in this order. Anyhow the only necesssary phase is indeed the first one. In fact if in the square example the true active set is known from the beginning, for the half-circle is discovered after a while. So for the square case, III) follows I), while for the semicircle, we can appreciate two different situations: I) followed by II) and I) followed by III).
Regarding Hertzian contact, in all cases the rate of convergence has a non linear behaviour at the beginning and at the end becomes constant. Since there is only one phase in which the rate is constant, after I) we have either II) or III), but not both. Essentially the third phase concerns a), b) for $\lambda = 1, \infty$ and for all meshes and c), d) only for $\lambda = 1$ in the uniform case. Nevertheless generally the convergence for c) and d) is slow. For c), this happens because the coarse constraints are so strict that we have I) and II), while III) is never approached; in the d) case, on the other hand, we have no control of the coarse constraints and therefore the convergence is not even ensured. If a good convergence rate is achieved in the uniform case, $\lambda = 1$, it is probably due to the small number of degrees on the contact boundary and the compressibility of the material: we need very few iterations to detect the active degrees of freedom.
Thus it is evident that it is desirable to avoid c) and d), since III) is difficult to reach and therefore the convergence rates tend to be very large. The c) and d) cases behave similarly. The c) case needs the implementation of the non-linear projection, but ensures reduction of the energy. In a complementary way, the d) approach does not need any non-linear projection, but does not guarantee energy reduction.
As opposed to c) and d), a) and b) facilitate the access to the linear setting with a very similar speed of convergence. Anyhow for a) it is necessary to know the coarse edges of the patch and also which is the corresponding fine midpoint. For b), instead, only the external nodes on the fine nodes patch are needed. This suggests to prefer b) and avoid the use of a). Indeed, among all, the b) case is the one which actually minimizes the functional, requires less effort of programming, and is sufficiently fast.

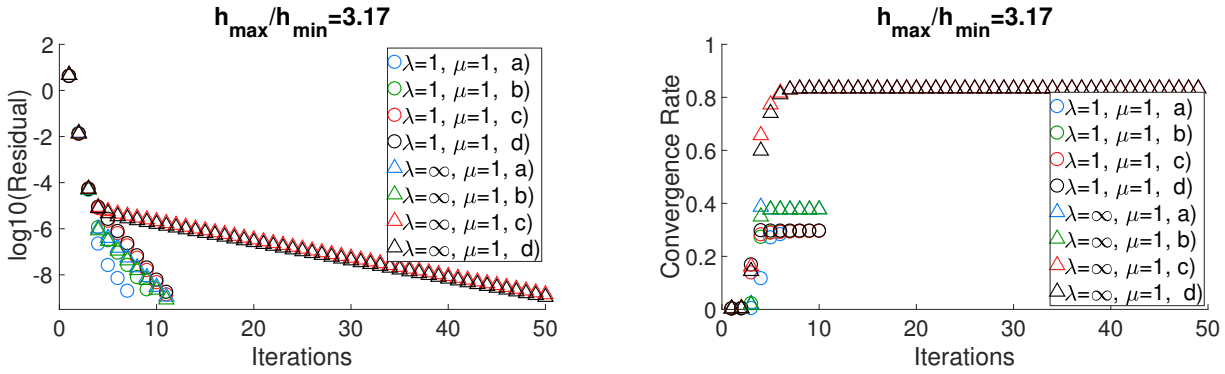

Figure 4: Mesh with $h_{max}/h_{min} = 3.1688$. Where:
a) projection (25), b)projection (27), c)projection (28), d)coarse constraints=∞.

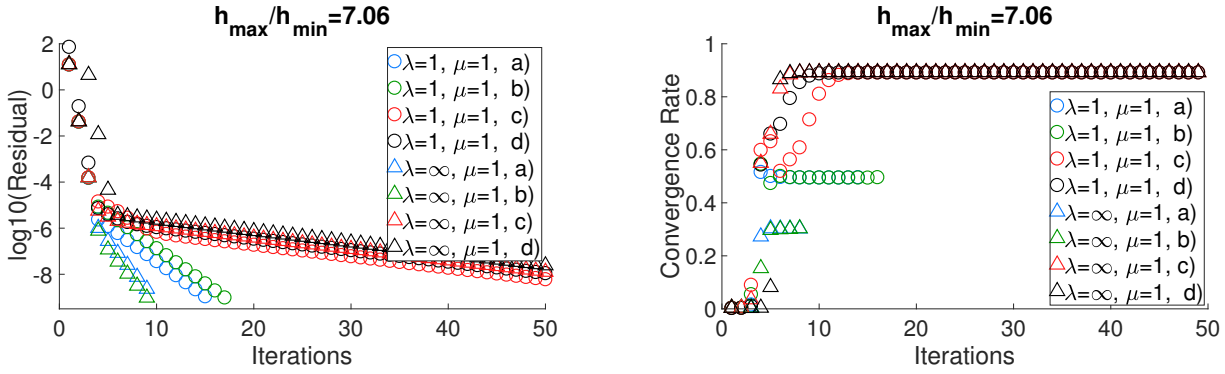

Figure 5: Mesh with $h_{max}/h_{min} = 7.0567$. Where:
a)projection (25), b)projection (27), c)projection (28), d)coarse constraints=∞.

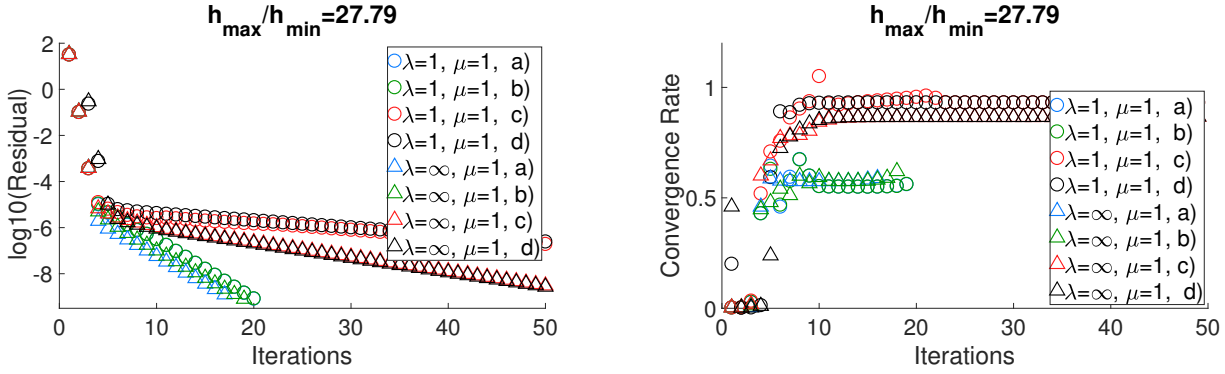

Figure 6: Mesh with $h_{max}/h_{min} = 29.7936$. Where:
a)projection (25), b)projection (27), c)projection (28), d)coarse constraints=∞.

References

[1] Analysis of first-order system least squares (fosls) for elliptic problems with discontinuous coefficients: Part I, author=Berndt, Markus and Manteuffel, Thomas A and McCormick, Stephen F and Starke, Gerhard, journal=SIAM Journal on Numerical Analysis, volume=43, number=1, pages=386–408, year=2005, publisher=SIAM.

[2] Douglas Arnold, Richard Falk, and Ragnar Winther. Preconditioning in H(div) and applications. *Mathematics of Computation of the American Mathematical Society*, 66(219):957–984, 1997.

[3] Douglas N Arnold, Richard S Falk, and Ragnar Winther. Multigrid in H(div) and H(curl). *Numerische Mathematik*, 85(2):197–217, 2000.

[4] Ragnar Winther Arnold Douglas, Richard S. Falk. Multigrid preconditioning in H(div) on non-convex polygons.

[5] Lori Badea. Convergence rate of a multiplicative schwarz method for strongly nonlinear variational inequalities. In *IFIP International Information Security Conference*, pages 31–41. Springer, 2002.

[6] Lori Badea. Global convergence rate of a standard multigrid method for variational inequalities. *IMA Journal of Numerical Analysis*, 34(1):197–216, 2014.

[7] Lori Badea and Rolf Krause. One-and two-level schwarz methods for variational inequalities of the second kind and their application to frictional contact. *Numerische Mathematik*, 120(4):573–599, 2012.

[8] Harald Bader and Ronald HW Hoppe. *Multigrid solution of Signorini type problems in contact elastostatics*. Bibliothek der Fak. Mathematik und Informatik, Technische Univ., 1993.

[9] Markus Berndt, Thomas A Manteuffel, and Stephen F McCormick. Local error estimates and adaptive refinement for first-order system least squares (FOSLS). *Electron. Trans. Numer. Anal*, 6:35–43, 1997.

[10] Pavel B Bochev and Max D Gunzburger. *Least-squares finite element methods*, volume 166. Springer Science & Business Media, 2009.

[11] Franco Brezzi and Michel Fortin. *Mixed and hybrid finite element methods*, volume 15. Springer Science & Business Media, 2012.

[12] Zhiqiang Cai and Gerhard Starke. Least-squares methods for linear elasticity. *SIAM Journal on Numerical Analysis*, 42(2):826–842, 2004.

[13] Philippe G Ciarlet. The finite element method for elliptic problems. *Classics in applied mathematics*, 40:1–511, 2002.

[14] Ivar Ekeland and Roger Temam. *Convex analysis and variational problems*, volume 28. Siam, 1999.

[15] E Gelman and J Mandel. On multilevel iterative methods for optimization problems. *Mathematical Programming*, 48(1-3):1–17, 1990.

[16] Ralf Hiptmair. Multigrid method for H(div) in three dimensions. *Electron. Trans. Numer. Anal*, 6(1):133–152, 1997.

[17] Ralf Hiptmair and Jinchao Xu. Nodal auxiliary space preconditioning in H(curl) and H(div) spaces. *SIAM Journal on Numerical Analysis*, 45(6):2483–2509, 2007.

[18] Noboru Kikuchi and John Tinsley Oden. *Contact problems in elasticity: a study of variational inequalities and finite element methods*, volume 8. siam, 1988.

[19] Tzanio V Kolev and Panayot S Vassilevski. Parallel auxiliary space amg solver for H(div) problems. *SIAM Journal on Scientific Computing*, 34(6):A3079–A3098, 2012.

[20] Ralf Kornhuber. Monotone multigrid methods for elliptic variational inequalities i. *Numerische Mathematik*, 69(2):167–184, 1994.

[21] Ralf Kornhuber and Rolf Krause. Adaptive multigrid methods for Signorini's problem in linear elasticity. *Computing and Visualization in Science*, 4(1):9–20, 2001.

[22] Ralf Kornhuber, Rolf Krause, O Sander, P Deuflhard, and S Ertel. A monotone multigrid solver for two body contact problems in biomechanics. *Computing and Visualization in Science*, 11(1):3–15, 2008.

[23] Rolf Krause, Benjamin Müller, and Gerhard Starke. An adaptive least-squares mixed finite element method for the Signorini problem. *Numerical Methods for Partial Differential Equations*, 33(1):276–289, 2017.

[24] Rolf Krause, Alessandro Rigazzi, and Johannes Steiner. A parallel multigrid method for constrained minimization problems and its application to friction, contact, and obstacle problems. *Computing and Visualization in Science*, 18(1):1–15, 2016.

[25] Jan Mandel. A multilevel iterative method for symmetric, positive definite linear complementarity problems. *applied mathematics and optimization*, 11(1):77–95, 1984.

[26] Gerhard Starke. Gauss-Newton multilevel methods for least-squares finite element computations of variably saturated subsurface flow. *Computing*, 64(4):323–338, 2000.

[27] Gerhard Starke. An adaptive least-squares mixed finite element method for elasto-plasticity. *SIAM Journal on Numerical Analysis*, 45(1):371–388, 2007.

[28] Jinchao Xu, Long Chen, and Ricardo H Nochetto. Optimal multilevel methods for H(grad), H(curl), and H(div) systems on graded and unstructured grids. In *Multiscale, nonlinear and adaptive approximation*, pages 599–659. Springer, 2009.

[29] Suh-Yuh Yang and Jinn-Liang Liu. Least-squares finite element methods for the elasticity problem. *Journal of computational and applied mathematics*, 87(1):39–60, 1997.